63 (2018) APPLICATIONS OF MATHEMATICS No. 6, 739–764

SPACE-TIME DISCONTINUOUS GALERKIN METHOD FOR THE SOLUTION OF FLUID-STRUCTURE INTERACTION

Monika Balázsová, Miloslav Feistauer, Jaromír Horáček, Martin Hadrava, Adam Kosík, Praha

Received May 2, 2018. Published online November 19, 2018.

Abstract. The paper is concerned with the application of the space-time discontinuous Galerkin method (STDGM) to the numerical solution of the interaction of a compressible flow and an elastic structure. The flow is described by the system of compressible Navier-Stokes equations written in the conservative form. They are coupled with the dynamic elasticity system of equations describing the deformation of the elastic body, induced by the aerodynamical force on the interface between the gas and the elastic structure. The domain occupied by the fluid depends on time. It is taken into account in the Navier-Stokes equations rewritten with the aid of the arbitrary Lagrangian-Eulerian (ALE) method. The resulting coupled system is discretized by the STDGM using piecewise polynomial approximations of the sought solution both in space and time. The developed method can be applied to the solution of the compressible flow for a wide range of Mach numbers and Reynolds numbers. For the simulation of elastic deformations two models are used: the linear elasticity model and the nonlinear neo-Hookean model. The main goal is to show the robustness and applicability of the method to the simulation of the air flow in a simplified model of human vocal tract and the flow induced vocal folds vibrations. It will also be shown that in this case the linear elasticity model is not adequate and it is necessary to apply the nonlinear model.

Keywords: nonstationary compressible Navier-Stokes equations; time-dependent domain; arbitrary Lagrangian-Eulerian method; linear and nonlinear dynamic elasticity; space-time discontinuous Galerkin method; vocal folds vibrations

MSC 2010: 65M60, 65M99, 74B05, 74B20, 74F10

The research was supported by the grant 17-01747S (M. Feistauer, M. Hadrava) and the grant 16-01246S (J. Horáček) of the Czech Science Foundation, and the research of M. Balázsová was supported by the Charles University, project SVV-2017-260455.

DOI: 10.21136/AM.2018.0139-18

1. Introduction

In some problems of science and technology it is necessary to solve partial differential equations in time-dependent domains. Particularly, we can mention problems of fluid-structure interaction (FSI), when the boundary of the domain occupied by the moving fluid is deformed in dependence on time according to the deformation of an elastic body adjacent to the fluid. There are several techniques how to solve numerically initial-boundary value problems in time-dependent domains. We can mention, e.g. the immersed boundary method or the fictitious domain method (see [5], [34]). Another, rather popular technique is the arbitrary Lagrangian-Eulerian (ALE) method (see [18]) based on an ALE mapping of a reference configuration onto a current configuration.

In the present paper, compressible flow in a time-dependent domain coupled with an elastic body is studied. The flow is described by the compressible Navier-Stokes equations written in the ALE form using conservative variables. It is coupled with the dynamic elasticity system describing the deformation of an elastic body, induced by the aerodynamical force on the interface between the gas and the elastic body. Both the flow and structural problems are discretized by the space-time discontinuous Galerkin method (STDGM). This means that the space as well as the time discretization is realized by piecewise polynomial functions depending on the space variables and on time.

In several works (see [9], [10], [25], [26], [29], [33]) we used the ALE method with success for the numerical solution of the compressible Navier-Stokes equations in the framework of FSI problems. The space discretization was carried out by the discontinuous Galerkin method (DGM). For the time discretization we used either the backward difference formula (BDF) or the DGM in time. In the latter case, we get the STDGM.

The discontinuous Galerkin time discretization was introduced and analyzed, e.g. in [19] for the solution of ordinary differential equations. In [1], [11], [20], [21], [36] and [37] the solution of parabolic problems is carried out with the aid of conforming finite elements in space combined with the DG time discretization. See also the monograph [38]. In [24], the STDGM was analyzed for a linear nonstationary convection-diffusion-reaction problem. The paper [28] is devoted to the theory of error estimates for the STDGM applied to a nonstationary convection-diffusion problem with a nonlinear convection and linear diffusion. In paper [8], the theory of the STDGM was developed for the case with nonlinear convection as well as diffusion. The paper [4] is a continuation of the works [28] and [8] by proving unconditional stability of the STDGM. In all the above mentioned theoretical papers, the space domain is independent of time.

There are several papers devoted to the analysis of linear convection-diffusion problems in time-dependent domains, formulated with the aid of the ALE method. We can mention [31], [32], and [7]. The latter paper is concerned with the stability analysis of the time DGM without space discretization. In [3] the stability of the STDGM applied to the solution of a scalar nonlinear convection-diffusion problem in a time-dependent domain was analyzed.

As follows from the above, the novelty of the presented work is the development and application of the STDGM to the solution of the compressible Navier-Stokes equations in the conservative ALE form in a time-dependent domain coupled with the linear or nonlinear neo-Hookean elasticity. The developed method is applied to the numerical simulation of air flow in a simplified model of human vocal tract and flow induced vocal folds vibrations.

In Section 2, the flow problem, elasticity problem and their coupling are formulated. Section 3 describes the STDGM discretization of the coupled problem, including the iterative algorithm of the realization of the discrete problem. Section 4 is devoted to algorithmization and numerical realization of the coupled problem and finally Section 5 presents numerical experiments showing the robustness of the developed method.

2. Formulation of the continuous problem

In what follows we describe nonstationary viscous compressible flow in time-dependent domains, the equations of dynamic linear and nonlinear elasticity and their coupling.

2.1. Compressible Navier-Stokes equations in a time-dependent domain.

We consider compressible flow in a bounded domain $\Omega_t \subset \mathbb{R}^2$ with Lipschitz boundary depending on time $t \in [0, T]$.

The dependence of the domain Ω_t on time is taken into account with the use of the *arbitrary Lagrangian-Eulerian* (ALE) method, see e.g. [10] or [9]. It is based on a regular one-to-one ALE mapping of the reference configuration Ω_0 onto the current configuration Ω_t:

$$\mathcal{A}_t \colon \overline{\Omega}_0 \to \overline{\Omega}_t, \text{ i.e., } \boldsymbol{X} \in \overline{\Omega}_0 \mapsto \boldsymbol{x} = \boldsymbol{x}(\boldsymbol{X}, t) = \mathcal{A}_t(\boldsymbol{X}) \in \overline{\Omega}_t. \tag{2.1}$$

We define the domain velocity

$$\begin{aligned} \tilde{\boldsymbol{z}}(\boldsymbol{X}, t) &= \frac{\partial}{\partial t}\mathcal{A}_t(\boldsymbol{X}), \\ \boldsymbol{z}(\boldsymbol{x}, t) &= \tilde{\boldsymbol{z}}(\mathcal{A}_t^{-1}(\boldsymbol{x}), t), \quad t \in [0, T], \ \boldsymbol{X} \in \Omega_0, \ \boldsymbol{x} \in \Omega_t, \end{aligned} \tag{2.2}$$

and the ALE derivative of the vector function $\boldsymbol{w} = \boldsymbol{w}(\boldsymbol{x}, t)$ defined for $\boldsymbol{x} \in \Omega_t$ and $t \in [0, T]$:

$$\frac{D^A}{Dt}\boldsymbol{w}(\boldsymbol{x}, t) = \frac{\partial \widetilde{\boldsymbol{w}}}{\partial t}(\boldsymbol{X}, t), \tag{2.3}$$

where

$$\widetilde{\boldsymbol{w}}(\boldsymbol{X}, t) = \boldsymbol{w}(\mathcal{A}_t(\boldsymbol{X}), t), \quad \boldsymbol{X} \in \Omega_0, \quad \boldsymbol{x} = \mathcal{A}_t(\boldsymbol{X}). \tag{2.4}$$

The system describing the compressible flow, consisting of the continuity equation, the Navier-Stokes equations and the energy equation, can be written in the form

$$\frac{\partial \boldsymbol{w}}{\partial t} + \sum_{s=1}^{2} \frac{\partial \boldsymbol{f}_s(\boldsymbol{w})}{\partial x_s} = \sum_{s=1}^{2} \frac{\partial \boldsymbol{R}_s(\boldsymbol{w}, \nabla \boldsymbol{w})}{\partial x_s}. \tag{2.5}$$

Then, using the relations

$$\frac{D^A w_i}{Dt} = \frac{\partial w_i}{\partial t} + \operatorname{div}(\boldsymbol{z} w_i) - w_i \operatorname{div} \boldsymbol{z}, \quad i = 1, \dots, 4, \tag{2.6}$$

we can write system (2.5) in the ALE form

$$\frac{D^A \boldsymbol{w}}{Dt} + \sum_{s=1}^{2} \frac{\partial \boldsymbol{g}_s(\boldsymbol{w})}{\partial x_s} + \boldsymbol{w} \operatorname{div} \boldsymbol{z} = \sum_{s=1}^{2} \frac{\partial \boldsymbol{R}_s(\boldsymbol{w}, \nabla \boldsymbol{w})}{\partial x_s}, \tag{2.7}$$

see for example [9]. Here

$$\begin{aligned}
\boldsymbol{w} &= (w_1, \dots, w_4)^\top = (\varrho, \varrho v_1, \varrho v_2, E)^\top \in \mathbb{R}^4, \\
\boldsymbol{w} &= \boldsymbol{w}(\boldsymbol{x}, t), \ \boldsymbol{x} \in \Omega_t, \ t \in (0, T), \\
\boldsymbol{g}_s(\boldsymbol{w}) &= \boldsymbol{f}_s(\boldsymbol{w}) - z_s \boldsymbol{w}, \quad s = 1, 2, \\
\boldsymbol{f}_s(\boldsymbol{w}) &= (f_{s1}, \dots, f_{s4})^\top = (\varrho v_s, \varrho v_1 v_s + \delta_{1s}\, p, \varrho v_2 v_s + \delta_{2s}\, p, (E + p) v_s)^\top, \\
\boldsymbol{R}_s(\boldsymbol{w}, \nabla \boldsymbol{w}) &= (R_{s1}, \dots, R_{s4})^\top = (0, \tau_{s1}^V, \tau_{s2}^V, \tau_{s1}^V\, v_1 + \tau_{s2}^V\, v_2 + \kappa \partial \theta / \partial x_s)^\top, \\
\tau_{ij}^V &= \lambda \operatorname{div} \boldsymbol{v}\, \delta_{ij} + 2\mu\, d_{ij}(\boldsymbol{v}), \quad d_{ij}(\boldsymbol{v}) = \frac{1}{2}\Big(\frac{\partial v_i}{\partial x_j} + \frac{\partial v_j}{\partial x_i}\Big).
\end{aligned} \tag{2.8}$$

We use the following notation: ϱ—fluid density, p—pressure, E—total energy, $\boldsymbol{v} = (v_1, v_2)$—flow velocity, θ—absolute temperature, $\gamma > 1$—Poisson adiabatic constant, $c_v > 0$—specific heat at constant volume, $\mu > 0$, $\lambda = -2\mu/3$—fluid viscosity coefficients, κ—heat conduction, τ_{ij}^V—components of the viscous part of the aerodynamical stress tensor. The above system is completed by the thermodynamical relations

$$p = (\gamma - 1)\Big(E - \frac{1}{2}\varrho |\boldsymbol{v}|^2\Big), \quad \theta = \frac{1}{c_v}\Big(\frac{E}{\varrho} - \frac{1}{2}|\boldsymbol{v}|^2\Big). \tag{2.9}$$

It is possible to show that

$$\boldsymbol{f}_s(\boldsymbol{w}) = \mathbb{A}_s(\boldsymbol{w})\boldsymbol{w}, \quad \boldsymbol{R}_s(\boldsymbol{w}, \nabla \boldsymbol{w}) = \sum_{k=1}^{2} \mathbb{K}_{s,k}(\boldsymbol{w}) \frac{\partial \boldsymbol{w}}{\partial x_k}, \quad s = 1, 2, \tag{2.10}$$

where

$$\mathbb{A}_s(\boldsymbol{w}) = \frac{D\boldsymbol{f}_s(\boldsymbol{w})}{D\boldsymbol{w}}, \quad s = 1, 2,$$

are the Jacobi matrices of the mappings $\boldsymbol{f}_s$ and $\mathbb{K}_{s,k}(\boldsymbol{w}) \in \mathbb{R}^{4\times 4}$ are matrices depending nonlinearly on $\boldsymbol{w}$ (cf., e.g., [16]).

We assume that the boundary $\partial\Omega_t$ of the domain Ω_t is formed by disjoint parts Γ_I—inlet through which the fluid flows into the domain Ω_t, Γ_O—outlet through which the fluid leaves Ω_t, and Γ_{W_t}—impermeable walls the parts of which can depend on time t. We assume that Γ_I and Γ_O are fixed (see Figure 1).

The resulting system is equipped with the initial condition $\boldsymbol{w}(x, 0) = \boldsymbol{w}^0(x)$, $x \in \Omega_0$, and the boundary conditions

$$\begin{aligned}
&\text{a) } \varrho = \varrho_D && \text{on } \Gamma_I,\\
&\text{b) } \boldsymbol{v} = \boldsymbol{v}_D = (v_{D1}, v_{D2})^\top && \text{on } \Gamma_I,\\
&\text{c) } \sum_{i,j=1}^{2} \tau_{ij}^V n_i v_j + k\frac{\partial \theta}{\partial \boldsymbol{n}} = 0 && \text{on } \Gamma_I,\\
&\text{d) } \boldsymbol{v} = \boldsymbol{z}_D = \text{velocity of a wall } \Gamma_{W_t},\\
&\text{e) } \frac{\partial \theta}{\partial \boldsymbol{n}} = 0 && \text{on } \Gamma_{W_t},\\
&\text{f) } \sum_{i=1}^{2} \tau_{ij}^V n_i = 0, && j = 1, 2, \text{ on } \Gamma_O,\\
&\text{g) } \frac{\partial \theta}{\partial \boldsymbol{n}} = 0 && \text{on } \Gamma_O,
\end{aligned} \tag{2.11}$$

with prescribed data ϱ_D, $\boldsymbol{v}_D$ and $\boldsymbol{z}_D$. Here $\boldsymbol{n} = (n_1, n_2)$ denotes the outward unit normal to $\partial\Omega_t$ and $\partial/\partial\boldsymbol{n}$ is the derivative in the direction $\boldsymbol{n}$. On Γ_O and Γ_{W_t} only three boundary conditions are specified. The missing condition is completed in the discrete problem by extrapolation, see (3.9)–(3.11).

2.2. Dynamic elasticity system. We assume that the elastic body is represented by a bounded polygonal domain $\Omega^b \subset \mathbb{R}^2$ with boundary $\partial\Omega^b = \Gamma_D^b \cup \Gamma_N^b$, where $\Gamma_D^b \cap \Gamma_N^b = \emptyset$. On Γ_D^b and Γ_N^b we prescribe the Dirichlet and the Neumann boundary condition, respectively. The deformation of the body is described by the displacement $\boldsymbol{u}\colon\ \Omega^b \times [0, T] \to \mathbb{R}^2$ and the deformation mapping

$$\boldsymbol{\psi}(\boldsymbol{X}, t) = \boldsymbol{X} + \boldsymbol{u}(\boldsymbol{X}, t), \quad \boldsymbol{X} \in \Omega^b,\ t \in [0, T]. \tag{2.12}$$

Further, we introduce the deformation gradient, the Jacobian and the cofactor Cof $\boldsymbol{F}$ of the matrix $\boldsymbol{F}$:

$$\boldsymbol{F} = \nabla \boldsymbol{\psi}, \quad J = \det \boldsymbol{F} > 0, \quad \operatorname{Cof} \boldsymbol{F} = J(\boldsymbol{F}^{-\top}). \tag{2.13}$$

Here $\boldsymbol{F}^{-\top} = (\boldsymbol{F}^{-1})^{-\top}$. Further, we introduce the first Piola-Kirchhoff stress tensor $\boldsymbol{P}$. Its form depends on the chosen elasticity model (cf. [13]).

The general dynamic elasticity problem is formulated in the following way: Find a displacement function $\boldsymbol{u}\colon\ \Omega^b \times [0,T] \to \mathbb{R}^2$ such that

$$\varrho^b \frac{\partial^2 \boldsymbol{u}}{\partial t^2} + c_M \varrho^b \frac{\partial \boldsymbol{u}}{\partial t} - \operatorname{div} \boldsymbol{P}(\boldsymbol{F}) = \boldsymbol{f} \quad \text{in } \Omega^b \times [0,T], \tag{2.14}$$

$$\boldsymbol{u} = \boldsymbol{u}_D \quad \text{in } \Gamma_D^b \times [0,T], \tag{2.15}$$

$$\boldsymbol{P}(\boldsymbol{F})\, \boldsymbol{n} = \boldsymbol{g}_N \quad \text{in } \Gamma_N^b \times [0,T], \tag{2.16}$$

$$\boldsymbol{u}(\cdot,0) = \boldsymbol{u}_0, \quad \frac{\partial \boldsymbol{u}}{\partial t}(\cdot,0) = \boldsymbol{y}_0 \quad \text{in } \Omega^b, \tag{2.17}$$

where $\boldsymbol{f}\colon\ \Omega^b \times [0,T] \to \mathbb{R}^2$ is the density of the acting volume force, $\boldsymbol{g}_N\colon\ \Gamma_N^b \times [0,T] \to \mathbb{R}^2$ is the surface traction, $\boldsymbol{u}_D\colon\ \Gamma_D^b \times [0,T] \to \mathbb{R}^2$ is the prescribed displacement, $\boldsymbol{u}_0\colon\ \Omega^b \to \mathbb{R}^2$ is the initial displacement, $\boldsymbol{y}_0\colon\ \Omega^b \to \mathbb{R}^2$ is the initial deformation velocity, $\varrho^b > 0$ is the material density, and $c_M \geqslant 0$ is the damping coefficient.

In the stationary case (static problem) we seek $\boldsymbol{u}\colon\ \Omega^b \to \mathbb{R}^2$ such that

$$-\operatorname{div} \boldsymbol{P}(\boldsymbol{F}) = \boldsymbol{f} \quad \text{in } \Omega^b, \tag{2.18}$$

$$\boldsymbol{u} = \boldsymbol{u}_D \quad \text{on } \Gamma_D^b, \quad \boldsymbol{P}(\boldsymbol{F})\boldsymbol{n} = \boldsymbol{g}_N \quad \text{on } \Gamma_N^b. \tag{2.19}$$

2.2.1. Linear elasticity. In case of linear elasticity the stress tensor $\boldsymbol{P}(\boldsymbol{F})$ is denoted as $\boldsymbol{\sigma}(\boldsymbol{u})$, which depends linearly on the strain tensor $\boldsymbol{e}(\boldsymbol{u}) = (\nabla \boldsymbol{u} + \nabla \boldsymbol{u}^{\top})/2$ according to the relation

$$\boldsymbol{P}(\boldsymbol{F}) := \boldsymbol{\sigma}(\boldsymbol{u}) = \lambda^b \operatorname{tr}(\boldsymbol{e}(\boldsymbol{u}))\mathbb{I} + 2\mu^b \boldsymbol{e}(\boldsymbol{u}). \tag{2.20}$$

Here λ^b and μ^b are the Lamé parameters that can be expressed with the aid of the Young modulus E^b and the Poisson ratio ν^b:

$$\lambda^b = \frac{E^b \nu^b}{(1+\nu^b)(1-2\nu^b)}, \quad \mu^b = \frac{E^b}{2(1+\nu^b)}. \tag{2.21}$$

2.2.2. Nonlinear elasticity. In the nonlinear case we consider the model of neo-Hookean material with the stress tensor

$$\boldsymbol{P}(\boldsymbol{F}) = \mu^b(\boldsymbol{F} - \boldsymbol{F}^{-\top}) + \lambda^b \log(\det \boldsymbol{F})\boldsymbol{F}^{-\top}. \tag{2.22}$$

For a detailed description we can refer the reader to monographs [13] and [6].

2.3. Fluid-structure coupling. In the FSI problem the coupling of the discrete flow problem and the structural problem is realized via the transmission conditions representing the continuity of the velocity and the normal stress on the common boundary $\widetilde{\Gamma}_{W_t}$ between fluid and structure. We assume that

$$\widetilde{\Gamma}_{W_t} = \{\boldsymbol{x} \in \mathbb{R}^2;\ \boldsymbol{x} = \boldsymbol{X} + \boldsymbol{u}(\boldsymbol{X}, t),\ \boldsymbol{X} \in \Gamma_N^b\} \subset \Gamma_{W_t}. \tag{2.23}$$

Then we use the following transmission conditions:

a) For linear elasticity we assume that

$$\boldsymbol{\sigma}(\boldsymbol{u}(\boldsymbol{X}, t))\boldsymbol{n}(\boldsymbol{X}) = \boldsymbol{\tau}^f(\boldsymbol{x}, t)\boldsymbol{n}(\boldsymbol{X}), \quad \boldsymbol{v}(\boldsymbol{x}, t) = \frac{\partial \boldsymbol{u}(\boldsymbol{X}, t)}{\partial t}. \tag{2.24}$$

b) For nonlinear elasticity we use the conditions

$$\boldsymbol{P}(\boldsymbol{F}(\boldsymbol{X}, t))\boldsymbol{n}(\boldsymbol{X}) = \boldsymbol{\tau}^f(\boldsymbol{x}, t)\,\mathrm{Cof}(\boldsymbol{F}(\boldsymbol{X}, t))\boldsymbol{n}(\boldsymbol{X}),\ \boldsymbol{v}(\boldsymbol{x}, t) = \frac{\partial \boldsymbol{u}(\boldsymbol{X}, t)}{\partial t}. \tag{2.25}$$

In the above relations, $\boldsymbol{x} = \boldsymbol{X} + \boldsymbol{u}(\boldsymbol{X}, t)$, $\boldsymbol{X} \in \Gamma_N^b$, $\boldsymbol{x} \in \widetilde{\Gamma}_{Wt}$, the expression $\boldsymbol{\tau}^f = \{\tau_{ij}^f\}_{i,j=1}^2 = \{-p\delta_{ij} + \tau_{ij}^V\}_{i,j=1}^2$ represents the aerodynamical stress tensor and $\boldsymbol{n}(\boldsymbol{X})$ is the unit outward normal to $\partial\Omega^b$ on Γ_N^b (by δ_{ij} we denote the Kronecker symbol).

2.4. Determination of the ALE mapping. The ALE mapping $\mathcal{A}_t$ is determined with the aid of an artificial stationary linear elasticity problem proposed in [40]. We seek $\boldsymbol{d} = (d_1, d_2)$ defined in Ω_0 as a solution of the elastic static system

$$\sum_{j=1}^{2} \frac{\partial \tau_{ij}^a(\boldsymbol{d})}{\partial X_j} = 0 \quad \text{in } \Omega_0,\ i = 1, 2, \tag{2.26}$$

where τ_{ij}^a are the components of the artificial stress tensor

$$\tau_{ij}^a = \delta_{ij}\lambda^a \operatorname{div} \boldsymbol{d} + 2\mu^a e_{ij}^a(\boldsymbol{d}), \quad e_{ij}^a(\boldsymbol{d}) = \frac{1}{2}\Big(\frac{\partial d_i}{\partial X_j} + \frac{\partial d_j}{\partial X_i}\Big), \quad i = 1, 2.$$

The Lamé coefficients λ^a and μ^a are related to the artificial Young modulus E^a and the artificial Poisson number σ^a similarly to Section 2.2. The boundary conditions for $\boldsymbol{d}$ are prescribed by

$$\boldsymbol{d}|_{\Gamma_I \cup \Gamma_O} = 0, \quad \boldsymbol{d}|_{\Gamma_{W_0} \setminus \Gamma_N^b} = 0, \quad \boldsymbol{d}(\boldsymbol{X}, t) = \boldsymbol{u}(\boldsymbol{X}, t), \quad \boldsymbol{X} \in \Gamma_N^b. \tag{2.27}$$

The solution of the problem (2.26)–(2.27) gives us the ALE mapping of $\overline{\Omega}_0$ onto $\overline{\Omega}_t$ in the form

$$\mathcal{A}_t(\boldsymbol{X}) = \boldsymbol{X} + \boldsymbol{d}(\boldsymbol{X}, t), \quad \boldsymbol{X} \in \overline{\Omega}_0, \tag{2.28}$$

for each time instant t.

3. Discrete problem

The next section is devoted to the description of the STDGM discretization of the flow and structural problems.

3.1. Discretization of the flow problem (2.7)–(2.11)**.** We describe the discretization as it is carried out in the program system used in our practical computations. We assume that Ω_t is a polygonal domain for every $t \in [0, T]$. We denote by $\mathcal{T}_{ht}$ a partition of the closure $\overline{\Omega}_t$ into a finite number of closed triangles with disjoint interiors satisfying standard properties (see [12]). We suppose that $\mathcal{T}_{ht}$ is an image of $\mathcal{T}_{h0}$ under the regular mapping "$t \to \mathcal{A}_t$". Moreover, we assume that the ALE mapping $\mathcal{A}_t$ is continuous and affine in Ω_0.

By $\mathcal{F}_{ht}$ we denote the system of all faces of all elements $K \in \mathcal{T}_{ht}$. Further, we introduce the set of boundary faces $\mathcal{F}_{ht}^B = \{\Gamma \in \mathcal{F}_{ht};\ \Gamma \subset \partial\Omega_t\}$, the set of "Dirichlet" boundary faces $\mathcal{F}_{ht}^D = \{\Gamma \in \mathcal{F}_{ht}^B$ a Dirichlet condition is prescribed on $\Gamma\}$ and the set of inner faces $\mathcal{F}_{ht}^I = \mathcal{F}_{ht} \setminus \mathcal{F}_{ht}^B$. Each $\Gamma \in \mathcal{F}_{ht}$ is associated with a unit normal vector $\boldsymbol{n}_\Gamma$ to Γ. For $\Gamma \in \mathcal{F}_{ht}^B$ the normal $\boldsymbol{n}_\Gamma$ has the same orientation as the outer normal to $\partial\Omega_t$. We assume

For each $\Gamma \in \mathcal{F}_{ht}^I$ there exist two neighbouring elements $K_\Gamma^{(L)}, K_\Gamma^{(R)} \in \mathcal{T}_{ht}$ such that $\Gamma \subset \partial K_\Gamma^{(R)} \cap \partial K_\Gamma^{(L)}$. We use the convention that $K_\Gamma^{(R)}$ lies in the direction of $\boldsymbol{n}_\Gamma$ and $K_\Gamma^{(L)}$ lies in the opposite direction to $\boldsymbol{n}_\Gamma$. If $\Gamma \in \mathcal{F}_{ht}^B$, then the element adjacent to Γ will be denoted by $K_\Gamma^{(L)}$.

Now we introduce the space of piecewise polynomial functions

$$\boldsymbol{S}_{ht}^r = [S_{ht}^r]^4, \quad \text{with } S_{ht}^r = \{v;\ v|_K \in P_r(K)\ \forall K \in \mathcal{T}_{ht}\}, \tag{3.1}$$

where $r > 0$ is an integer and $P_r(K)$ denotes the space of all polynomials on K of degree $\leqslant r$. It is possible to see that $S_{ht}^r = \{v;\ v = \mathcal{A}_t(\hat{v}),\ \hat{v} \in S_{h0}^r\}$. A function $\boldsymbol{\varphi} \in \boldsymbol{S}_{ht}^r$ is, in general, discontinuous on interfaces $\Gamma \in \mathcal{F}_{ht}^I$. If $\boldsymbol{\varphi}$ is a function defined on $K_\Gamma^{(L)} \cup K_\Gamma^{(R)}$, then by $\boldsymbol{\varphi}_\Gamma^{(L)}$ and $\boldsymbol{\varphi}_\Gamma^{(R)}$ we denote the values of $\boldsymbol{\varphi}$ on Γ considered from the interior of $K_\Gamma^{(L)}$ and $K_\Gamma^{(R)}$, respectively (if these values make sense), and set $\langle\boldsymbol{\varphi}\rangle_\Gamma = (\boldsymbol{\varphi}_\Gamma^{(L)} + \boldsymbol{\varphi}_\Gamma^{(R)})/2$, $[\boldsymbol{\varphi}]_\Gamma = \boldsymbol{\varphi}_\Gamma^{(L)} - \boldsymbol{\varphi}_\Gamma^{(R)}$.

The discrete problem is derived in the following way: We multiply system (2.7) by a test function $\boldsymbol{\varphi}_h \in \boldsymbol{S}_{ht}^r$, integrate over $K \in \mathcal{T}_{ht}$, apply Green's theorem, sum over all elements $K \in \mathcal{T}_{ht}$, use the concept of the numerical flux and introduce suitable terms mutually vanishing for a regular exact solution and linearize the resulting forms on the basis of properties (2.10) of the functions $\boldsymbol{f}_s$ and $\boldsymbol{R}_s$. In this way we get the following forms (followed by the explanation of symbols appearing in their definitions):

$$
\begin{aligned}
(3.2)\qquad \hat{a}_h(\overline{\boldsymbol{w}}_h, \boldsymbol{w}_h, \boldsymbol{\varphi}_h, t) = {} & \sum_{K\in\mathcal{T}_{ht}} \int_K \sum_{s=1}^{2}\sum_{k=1}^{2} \mathbb{K}_{s,k}(\overline{\boldsymbol{w}}_h)\, \frac{\partial \boldsymbol{w}_h}{\partial x_k} \cdot \frac{\partial \boldsymbol{\varphi}_h}{\partial x_s}\,\mathrm{d}\boldsymbol{x} \\
& - \sum_{\Gamma\in\mathcal{F}_{ht}^I} \int_\Gamma \sum_{s=1}^{2} \Big\langle \sum_{k=1}^{2} \mathbb{K}_{s,k}(\overline{\boldsymbol{w}}_h) \frac{\partial \boldsymbol{w}_h}{\partial x_k} \Big\rangle (\boldsymbol{n}_\Gamma)_s \cdot [\boldsymbol{\varphi}_h]\,\mathrm{d}S \\
& - \sum_{\Gamma\in\mathcal{F}_{ht}^D} \int_\Gamma \sum_{s=1}^{2}\sum_{k=1}^{2} \mathbb{K}_{s,k}(\overline{\boldsymbol{w}}_h) \frac{\partial \boldsymbol{w}_h}{\partial x_k} (\boldsymbol{n}_\Gamma)_s \cdot \boldsymbol{\varphi}_h\,\mathrm{d}S \\
& - \Theta \sum_{\Gamma\in\mathcal{F}_{ht}^I} \int_\Gamma \sum_{s=1}^{2} \Big\langle \sum_{k=1}^{2} \mathbb{K}_{k,s}^{\top}(\overline{\boldsymbol{w}}_h) \frac{\partial \boldsymbol{\varphi}_h}{\partial x_k} \Big\rangle (\boldsymbol{n}_\Gamma)_s \cdot [\boldsymbol{w}_h]\,\mathrm{d}S \\
& - \Theta \sum_{\Gamma\in\mathcal{F}_{ht}^D} \int_\Gamma \sum_{s=1}^{2}\sum_{k=1}^{2} \mathbb{K}_{k,s}^{\top}(\overline{\boldsymbol{w}}_h) \frac{\partial \boldsymbol{\varphi}_h}{\partial x_k} (\boldsymbol{n}_\Gamma)_s \cdot \boldsymbol{w}_h\,\mathrm{d}S,
\end{aligned}
$$

$$
(3.3)\qquad d_h(\boldsymbol{w}_h, \boldsymbol{\varphi}_h, t) = \sum_{K\in\mathcal{T}_{ht}} \int_K (\boldsymbol{w}_h \cdot \boldsymbol{\varphi}_h)\,\mathrm{div}\,\boldsymbol{z}\,\mathrm{d}\boldsymbol{x},
$$

$$
(3.4)\qquad J_h(\boldsymbol{w}_h, \boldsymbol{\varphi}_h, t) = \sum_{\Gamma\in\mathcal{F}_{ht}^I} \int_\Gamma \frac{\mu C_W}{h_\Gamma} [\boldsymbol{w}_h] \cdot [\boldsymbol{\varphi}_h]\,\mathrm{d}S + \sum_{\Gamma\in\mathcal{F}_{ht}^D} \int_\Gamma \frac{\mu C_W}{h_\Gamma} \boldsymbol{w}_h \cdot \boldsymbol{\varphi}_h\,\mathrm{d}S,
$$

$$
\begin{aligned}
(3.5)\qquad l_h(\overline{\boldsymbol{w}}_h, \boldsymbol{w}_B, \boldsymbol{\varphi}_h, t) = {} & \sum_{\Gamma\in\mathcal{F}_{ht}^D} \int_\Gamma \frac{\mu C_W}{h_\Gamma} \boldsymbol{w}_B \cdot \boldsymbol{\varphi}_h\,\mathrm{d}S \\
& - \Theta \sum_{\Gamma\in\mathcal{F}_{ht}^D} \int_\Gamma \sum_{s=1}^{2}\sum_{k=1}^{2} \mathbb{K}_{k,s}^{T}(\overline{\boldsymbol{w}}_h) \frac{\partial \boldsymbol{\varphi}_h}{\partial x_k} (\boldsymbol{n}_\Gamma)_s \cdot \boldsymbol{w}_B\,\mathrm{d}S,
\end{aligned}
$$

$$
\begin{aligned}
(3.6)\qquad & \hat{b}_h(\overline{\boldsymbol{w}}_h, \boldsymbol{w}_h, \boldsymbol{\varphi}_h, t) \\
& = - \sum_{K\in\mathcal{T}_{ht_{k+1}}} \int_K \sum_{s=1}^{2} ((\mathbb{A}_s(\overline{\boldsymbol{w}}_h(x)) - z_s(x)\mathbb{I})\boldsymbol{w}_h(x)) \cdot \frac{\partial \boldsymbol{\varphi}_h(x)}{\partial x_s}\,\mathrm{d}\boldsymbol{x} \\
& \quad + \sum_{\Gamma\in\mathcal{F}_{ht}^I} \int_\Gamma (\mathbb{P}_g^+(\langle \overline{\boldsymbol{w}}_h\rangle_\Gamma, \boldsymbol{n}_\Gamma)\boldsymbol{w}_h^{(L)} + \mathbb{P}_g^-\big(\langle \overline{\boldsymbol{w}}_h\rangle_\Gamma, \boldsymbol{n}_\Gamma\big)\boldsymbol{w}_h^{(R)}) \cdot [\boldsymbol{\varphi}_h]\,\mathrm{d}S \\
& \quad + \sum_{\Gamma\in\mathcal{F}_{ht}^B} \int_\Gamma (\mathbb{P}_g^+\big(\langle \overline{\boldsymbol{w}}_h\rangle_\Gamma, \boldsymbol{n}_\Gamma\big)\boldsymbol{w}_h^{(L)} + \mathbb{P}_g^-(\langle \overline{\boldsymbol{w}}_h\rangle_\Gamma, \boldsymbol{n}_\Gamma)\overline{\boldsymbol{w}}_h^{(R)}) \cdot \boldsymbol{\varphi}_h\,\mathrm{d}S.
\end{aligned}
$$

We set $\Theta = 1$, $\Theta = 0$ or $\Theta = -1$ and get the so-called symmetric (SIPG), incomplete (IIPG) or nonsymmetric (NIPG) version, respectively, of the discretization of viscous terms. In (3.4) and (3.5), C_W denotes a positive sufficiently large constant.

In the form (3.6), symbols $\mathbb{P}_g^+(\boldsymbol{w},\boldsymbol{n})$ and $\mathbb{P}_g^-(\boldsymbol{w},\boldsymbol{n})$ denote the "positive" and "negative" parts of the matrix $\mathbb{P}_g(\boldsymbol{w},\boldsymbol{n}) = \sum\limits_{s=1}^{2}(\mathbb{A}_s(\boldsymbol{w}) - z_s\mathbb{I})n_s$ defined in the following way. By [23], this matrix is diagonalizable. It means that there exists a nonsingular matrix $\mathbb{T} = \mathbb{T}(\boldsymbol{w},\boldsymbol{n})$ such that

$$\mathbb{P}_g = \mathbb{T}\Lambda\mathbb{T}^{-1}, \quad \Lambda = \operatorname{diag}(\lambda_1,\dots,\lambda_4), \tag{3.7}$$

where $\lambda_i = \lambda_i(\boldsymbol{w},\boldsymbol{n})$ are eigenvalues of the matrix $\mathbb{P}_g$. Now we define the "positive" and "negative" parts of the matrix $\mathbb{P}_g$ by

$$\mathbb{P}_g^{\pm} = \mathbb{T}\Lambda^{\pm}\mathbb{T}^{-1}, \quad \Lambda^{\pm} = \operatorname{diag}(\lambda_1^{\pm},\dots,\lambda_4^{\pm}), \tag{3.8}$$

where $\lambda^+ = \max(\lambda,0)$, $\lambda^- = \min(\lambda,0)$.

The boundary state $\boldsymbol{w}_B$ is defined on the basis of the Dirichlet boundary conditions (2.11), a), b), d) and extrapolation:

$$\boldsymbol{w}_B = (\varrho_D, \varrho_D v_{D1}, \varrho_D v_{D2}, c_v\varrho_D\theta_\Gamma^{(L)} + \tfrac{1}{2}\varrho_D|\boldsymbol{v}_D|^2) \quad \text{on } \Gamma_I, \tag{3.9}$$

$$\boldsymbol{w}_B = \boldsymbol{w}_\Gamma^{(L)} \quad \text{on } \Gamma_O, \tag{3.10}$$

$$\boldsymbol{w}_B = (\varrho_\Gamma^{(L)}, \varrho_\Gamma^{(L)} z_{D1}, \varrho_\Gamma^{(L)} z_{D2}, c_v\varrho_\Gamma^{(L)}\theta_\Gamma^{(L)} + \tfrac{1}{2}\varrho_\Gamma^{(L)}|\boldsymbol{z}_D|^2) \quad \text{on } \Gamma_{Wt}. \tag{3.11}$$

For $\Gamma \in \mathcal{F}^B$ we set $\langle\overline{\boldsymbol{w}}_h\rangle_\Gamma = (\overline{\boldsymbol{w}}_\Gamma^{(L)} + \overline{\boldsymbol{w}}_\Gamma^{(R)})/2$ and the boundary state $\overline{\boldsymbol{w}}_\Gamma^{(R)}$ is defined with the aid of the solution of the 1D linearized initial-boundary Riemann problem as in [22].

In order to avoid spurious oscillations in the approximate solution in the vicinity of discontinuities or steep gradients, we apply artificial viscosity forms. They are based on the discontinuity indicator

$$g_t(K) = \frac{1}{h_K|K|^{3/4}}\int_{\partial K}[\overline{\varrho}_h]^2\,\mathrm{d}S, \quad K \in \mathcal{T}_{ht}, \tag{3.12}$$

introduced in [17]. By $[\overline{\varrho}_h]$ we denote the jump of the function $\overline{\varrho}_h$ on the boundary ∂K and $|K|$ denotes the area of the element K. Then we define the discrete discontinuity indicator $G_t(K) = 0$ if $g_t(K) < 1$, $G_t(K) = 1$ if $g_t(K) \geqslant 1$, and the artificial viscosity

forms (see [27])

$$\hat{\beta}_h(\overline{\boldsymbol{w}}_h, \boldsymbol{w}_h, \boldsymbol{\varphi}_h, t) = \nu_1 \sum_{K\in\mathcal{T}_{ht}} h_K G_t(K) \int_K \nabla \boldsymbol{w}_h \cdot \nabla \boldsymbol{\varphi}_h \,\mathrm{d}\boldsymbol{x}, \tag{3.13}$$

$$\hat{J}_h(\overline{\boldsymbol{w}}_h, \boldsymbol{w}_h, \boldsymbol{\varphi}_h, t) = \nu_2 \sum_{\Gamma\in\mathcal{F}_h^I} \frac{1}{2}(G_t(K_\Gamma^{(L)}) + G_t(K_\Gamma^{(R)})) \int_\Gamma [\boldsymbol{w}_h]\cdot[\boldsymbol{\varphi}_h]\,\mathrm{d}S,$$

with parameters ν_1, $\nu_2 = O(1)$.

Because of the time discretization we consider a partition $0 = t_0 < t_1 < \ldots < t_M = T$ of the time interval $[0,T]$ and denote $I_m = (t_{m-1}, t_m)$, $\tau_m = t_m - t_{m-1}$ for $m = 1,\ldots,M$, and $\tau = \max\limits_{m=1,\ldots,M} \tau_m$. We define the space $\boldsymbol{S}_{h\tau}^{rq} = [S_{h\tau}^{rq}]^4$, where

$$S_{h\tau}^{rq} = \left\{\phi;\ \phi(\boldsymbol{x},t) = \sum_{i=0}^{q} t^i \phi_i(\boldsymbol{x}),\ \phi_i \in S_{ht}^r,\ t\in I_m,\ \boldsymbol{x}\in\Omega_t,\ m = 1,\ldots,M\right\}, \tag{3.14}$$

with integers $r, q \geqslant 1$ and S_{ht}^r defined in (3.1). For $\boldsymbol{\varphi} \in \boldsymbol{S}_{h\tau}^{rq}$ we introduce the notation

$$\boldsymbol{\varphi}_m^\pm = \boldsymbol{\varphi}(t_m^\pm) = \lim_{t\to t_{m\pm}} \boldsymbol{\varphi}(t), \quad \{\boldsymbol{\varphi}\}_m = \boldsymbol{\varphi}_m^+ - \boldsymbol{\varphi}_m^-. \tag{3.15}$$

In order to bound the solution on intervals I_{m-1} and I_m, we augment the resulting identity by the penalty expression $(\{\boldsymbol{w}_{h\tau}\}_{m-1}, \boldsymbol{\varphi}_{h\tau}(t_{m-1}^+))_{t_{m-1}}$. The initial state $\boldsymbol{w}_{h\tau}(0-) \in \boldsymbol{S}_{h0}^r$ is defined as the $L^2(\Omega_{h0})$-projection of $\boldsymbol{w}^0$ on $\boldsymbol{S}_{h0}^r$, i.e.

$$(\boldsymbol{w}_{h\tau}(0-), \boldsymbol{\varphi}_h)_{\Omega_{t_0}} = (\boldsymbol{w}^0, \boldsymbol{\varphi}_h)_{\Omega_{t_0}} \quad \forall\, \boldsymbol{\varphi}_h \in \boldsymbol{S}_{h0}^r. \tag{3.16}$$

Moreover, we introduce the prolongation $\overline{\boldsymbol{w}}_{h\tau}(t)$ of $\boldsymbol{w}_{h\tau}|_{I_{m-1}}$ on the interval I_m. (The space-time DG technique with prolongation was analyzed theoretically in [39] on a scalar model problem.)

In what follows we denote

$$(a,b)_\omega = \int_\omega ab\,\mathrm{d}\boldsymbol{x} \tag{3.17}$$

for functions a, b defined in a set $\omega \subset \mathbb{R}^2$.

Now the *space-time DG approximate solution* is defined as a function $\boldsymbol{w}_{h\tau} \in \boldsymbol{S}_{h\tau}^{rq}$ satisfying (3.16) and the following relation for $m = 1, \dots, M$:

$$
\begin{aligned}
(3.18)\quad & \int_{I_m} \Big(\Big(\frac{D^{\mathcal{A}} \boldsymbol{w}_{h\tau}}{Dt}, \boldsymbol{\varphi}_{h\tau} \Big)_{\Omega_t} + \hat{a}_h(\overline{\boldsymbol{w}}_{h\tau}, \boldsymbol{w}_{h\tau}, \boldsymbol{\varphi}_{h\tau}, t) \Big) \, \mathrm{d}t \\
& \quad + \int_{I_m} (\hat{b}_h(\overline{\boldsymbol{w}}_{h\tau}, \boldsymbol{w}_{h\tau}, \boldsymbol{\varphi}_{h\tau}, t) + J_h(\boldsymbol{w}_{h\tau}, \boldsymbol{\varphi}_{h\tau}, t) + d_h(\boldsymbol{w}_{h\tau}, \boldsymbol{\varphi}_{h\tau}, t)) \, \mathrm{d}t \\
& \quad + \int_{I_m} (\hat{\beta}_h(\overline{\boldsymbol{w}}_{h\tau}, \boldsymbol{w}_{h\tau}, \boldsymbol{\varphi}_{h\tau}, t) + \hat{J}_h(\overline{\boldsymbol{w}}_{h\tau}, \boldsymbol{w}_{h\tau}, \boldsymbol{\varphi}_{h\tau}, t)) \, \mathrm{d}t \\
& \quad + (\{\boldsymbol{w}_{h\tau}\}_{m-1}, \boldsymbol{\varphi}_{h\tau}(t_{m-1}+))_{\Omega_{t_{m-1}}} \\
& = \int_{I_m} l_h(\overline{\boldsymbol{w}}_{h\tau}, \boldsymbol{w}_B, \boldsymbol{\varphi}_{h\tau}, t) \, \mathrm{d}t \quad \forall \, \boldsymbol{\varphi}_{h\tau} \in \boldsymbol{S}_{h\tau}^{rq}.
\end{aligned}
$$

R e m a r k 3.1. In the derivation of the discrete problem, the approximate solution and the test functions are viewed as elements of the space $\boldsymbol{S}_{h\tau}^{rq}$. In practical computations, integrals appearing in the definitions of the forms $\hat{a}_h, \hat{b}_h, d_h, J_h, \hat{J}_h$ and $\hat{\beta}_h$ and also the time integrals over I_m are evaluated with the aid of quadrature formulas using values of the approximate solution at discrete points of intervals I_m. Therefore, the space $\boldsymbol{S}_{h\tau}^{rq}$ is finite dimensional and the discrete problem is equivalent to a finite algebraic system for every $m = 1, \dots, M$.

3.2. Discretization of the elasticity problem. In the discretization of the structural problem we consider the displacement $\boldsymbol{u}$ and the deformation velocity $\boldsymbol{y}$ and split the basic system into two systems of first-order in time

$$
(3.19)\qquad \varrho^b \frac{\partial \boldsymbol{y}}{\partial t} + c_M \varrho^b \boldsymbol{y} - \operatorname{div} \boldsymbol{P}(\boldsymbol{F}) = \boldsymbol{f}, \quad \frac{\partial \boldsymbol{u}}{\partial t} - \boldsymbol{y} = 0 \quad \text{in } \Omega^b \times [0, T],
$$

$$
(3.20)\qquad \boldsymbol{u} = \boldsymbol{u}_D \quad \text{in } \Gamma_D^b \times [0, T],
$$

$$
(3.21)\qquad \boldsymbol{P}(\boldsymbol{F})\boldsymbol{n} = \boldsymbol{g}_N \quad \text{in } \Gamma_N^b \times [0, T],
$$

$$
(3.22)\qquad \boldsymbol{u}(\cdot, 0) = \boldsymbol{u}_0, \quad \boldsymbol{y}(\cdot, 0) = \boldsymbol{y}_0 \quad \text{in } \Omega^b.
$$

We construct a partition $\mathcal{T}_h^b$ of $\overline{\Omega}^b$ into a finite number of closed triangles K with mutually disjoint interiors satisfying the standard properties formulated in [12]. The approximate solution at every time instant $t \in [0, T]$ will be sought in the finite-dimensional space

$$
(3.23)\qquad \boldsymbol{S}_h^{b,s} = \{v \in L^2(\Omega);\ v|_K \in P_s(K), K \in \mathcal{T}_h^b\}^2,
$$

where $s > 0$ is an integer and $P_s(K)$ denotes the space of polynomials of degree not greater than s on K. By $\mathcal{F}_h^b$ we denote the system of all faces of all elements

$K \in \mathcal{T}_h^b$ and distinguish three sets of boundary, "Dirichlet", "Neumann" and inner faces: $\mathcal{F}_h^{b,B} = \{\Gamma \in \mathcal{F}_h^b;\ \Gamma \subset \partial\Omega^b\}$, $\mathcal{F}_h^{b,D} = \{\Gamma \in \mathcal{F}_h^b;\ \Gamma \subset \Gamma_b^D\}$, $\mathcal{F}_h^{b,N} = \{\Gamma \in \mathcal{F}_h^b;\ \Gamma \subset \Gamma_N^b\}$ and $\mathcal{F}_h^{b,I} = \mathcal{F}_h^b \setminus \mathcal{F}_h^{b,B}$. For each $\Gamma \in \mathcal{F}_h$ we define a unit normal vector $\boldsymbol{n}_\Gamma$. We assume that for $\Gamma \in \mathcal{F}_h^{b,B}$ the normal $\boldsymbol{n}_\Gamma$ has the same orientation as the outer normal to $\partial\Omega^b$. By h_Γ we denote the length of Γ. For $\boldsymbol{\varphi} \in \boldsymbol{S}_h^{b,s}$ symbols $\boldsymbol{\varphi}_\Gamma^{(L)}$ and $\boldsymbol{\varphi}_\Gamma^{(R)}$ denote the traces of $\boldsymbol{\varphi}$ on Γ from the sides of elements $K_\Gamma^{(L)}$ and $K_\Gamma^{(R)}$ adjacent to Γ. We assume that $\boldsymbol{n}_\Gamma$ is the outer normal to $\partial K_\Gamma^{(L)}$. Further, $\langle\boldsymbol{\varphi}\rangle_\Gamma$ denotes the average of the traces on Γ and $[\boldsymbol{\varphi}]_\Gamma = \boldsymbol{\varphi}_\Gamma^{(L)} - \boldsymbol{\varphi}_\Gamma^{(R)}$ is the jump of $\boldsymbol{\varphi}$ on Γ.

If $\boldsymbol{a} = (a_{ij})_{i,j=1}^2$, $\boldsymbol{b} = (b_{ij})_{i,j=1}^2$ are tensors, then we set $\boldsymbol{a} : \boldsymbol{b} = \sum\limits_{i,j=1}^{2} a_{ij} b_{ij}$.

The DG discretization in space is formulated with the use of following forms.

Linear elasticity form:

$$
\begin{aligned}
(3.24)\quad a_h^b(\boldsymbol{u},\boldsymbol{\varphi}) = {} & \sum_{K\in\mathcal{T}_h^b} \int_K \boldsymbol{\sigma}(\boldsymbol{u}) : \boldsymbol{e}(\boldsymbol{\varphi})\,\mathrm{d}\boldsymbol{x} - \sum_{\Gamma\in\mathcal{F}_h^{b,I}} \int_\Gamma (\langle\boldsymbol{\sigma}(\boldsymbol{u})\rangle\cdot\boldsymbol{n})\cdot[\boldsymbol{\varphi}]\,\mathrm{d}S \\
& - \sum_{\Gamma\in\mathcal{F}_h^{b,D}} \int_\Gamma (\boldsymbol{\sigma}(\boldsymbol{u})\cdot\boldsymbol{n})\cdot\boldsymbol{\varphi}\,\mathrm{d}S - \theta \sum_{\Gamma\in\mathcal{F}_h^{b,I}} \int_\Gamma (\langle\boldsymbol{\sigma}(\boldsymbol{\varphi})\rangle\cdot\boldsymbol{n})\cdot[\boldsymbol{u}]\,\mathrm{d}S \\
& - \theta \sum_{\Gamma\in\mathcal{F}_h^{b,D}} \int_\Gamma (\boldsymbol{\sigma}(\boldsymbol{\varphi})\cdot\boldsymbol{n})\cdot\boldsymbol{u}\,\mathrm{d}S,
\end{aligned}
$$

where $\boldsymbol{\sigma}(\boldsymbol{u})$ is defined by (2.20). Here the parameter θ is chosen as $1, 0, -1$ for the SIPG, IIPG, NIPG, respectively, version of the elasticity form.

Nonlinear IIPG elasticity form ($\theta = 0$):

$$
\begin{aligned}
(3.25)\qquad a_h^b(\boldsymbol{u},\boldsymbol{\varphi}) = {} & \sum_{K\in\mathcal{T}_h^b} \int_K \boldsymbol{P}(\boldsymbol{F}) : \nabla\boldsymbol{\varphi}\,\mathrm{d}\boldsymbol{x} - \sum_{\Gamma\in\mathcal{F}_h^{b,I}} \int_\Gamma (\langle\boldsymbol{P}(\boldsymbol{F})\rangle\boldsymbol{n})\cdot[\boldsymbol{\varphi}]\,\mathrm{d}S \\
& - \sum_{\Gamma\in\mathcal{F}_h^{b,D}} \int_\Gamma (\boldsymbol{P}(\boldsymbol{F})\boldsymbol{n})\cdot\boldsymbol{\varphi}\,\mathrm{d}S.
\end{aligned}
$$

Penalty form:

$$
(3.26)\qquad J_h^b(\boldsymbol{u},\boldsymbol{\varphi}) = \sum_{\Gamma\in\mathcal{F}_h^I} \int_\Gamma \frac{C_W^b}{h_\Gamma}[\boldsymbol{u}]\cdot[\boldsymbol{\varphi}]\,\mathrm{d}S + \sum_{\Gamma\in\mathcal{F}_h^D} \int_\Gamma \frac{C_W^b}{h_\Gamma}\boldsymbol{u}\cdot\boldsymbol{\varphi}\,\mathrm{d}S.
$$

Here $C_W^b > 0$ is a sufficiently large constant.

Right-hand side form:

$$
\begin{aligned}
l_h^b(\boldsymbol{\varphi})(t) = {} & \sum_{K\in\mathcal{T}_h^b}\int_K \boldsymbol{f}(t)\cdot\boldsymbol{\varphi}\,\mathrm{d}\boldsymbol{x} + \sum_{\Gamma\in\mathcal{F}_h^{b,N}}\int_\Gamma \boldsymbol{g}_N(t)\cdot\boldsymbol{\varphi}\,\mathrm{d}S \\
& - \theta\sum_{\Gamma\in\mathcal{F}_h^{b,D}}\int_\Gamma (\boldsymbol{\sigma}(\boldsymbol{\varphi})\boldsymbol{n})\cdot\boldsymbol{u}_D(t)\,\mathrm{d}S \\
& + \sum_{\Gamma\in\mathcal{F}_h^{b,D}}\int_\Gamma \frac{C_W^b}{h_\Gamma}\boldsymbol{u}_D(t)\cdot\boldsymbol{\varphi}\,\mathrm{d}S.
\end{aligned} \tag{3.27}
$$

Finally, we set $(\boldsymbol{u},\boldsymbol{\varphi})_{\Omega^b} = \int_{\Omega^b}\boldsymbol{u}\cdot\boldsymbol{\varphi}\,\mathrm{d}\boldsymbol{x}$. In the nonlinear case, it is not clear how to define the SIPG and NIPG versions of the elasticity forms so that the form a_h^b is linear with respect to the test function $\boldsymbol{\varphi}$.

3.2.1. STDGM for the structural problem. An approximate solution of problem (3.19)–(3.22), i.e., the approximations of the functions $\boldsymbol{u},\boldsymbol{y}$ will be sought in the space of piecewise polynomial vector functions $\boldsymbol{S}_{h\tau}^{b,sq^*} = [S_{h\tau}^{b,sq^*}]^2$, where

$$
\mathcal{V} = S_{h\tau}^{b,sq^*} = \Big\{ v\in L^2(\Omega^b\times(0,T));\ v|_{I_m} = \sum_{i=0}^{q^*} t^i\varphi_i \text{ with } \varphi_i\in S_h^{b,s},\ m=1,\dots,M\Big\}. \tag{3.28}
$$

By s and q^* we denote positive integers representing the degrees of polynomial approximations in space and time in the discretization of the structural problem. We introduce the one-sided limits and the jump of a function $\boldsymbol{\varphi}\in\boldsymbol{S}_{h\tau}^{b,sq^*}$ at time t_m similarly to (3.15). Now, the approximate STDG solution of problem (3.19)–(3.22) is defined as a couple $\boldsymbol{u}_{h\tau},\boldsymbol{y}_{h\tau}\in\boldsymbol{S}_{h\tau}^{b,sq^*}$ such that

$$
\begin{aligned}
\int_{I_m}\Big(\varrho^b\Big(\frac{\partial\boldsymbol{y}_{h\tau}}{\partial t},\boldsymbol{\varphi}_{h\tau}\Big)_{\Omega^b} & + c_M(\varrho^b\boldsymbol{y}_{h\tau},\boldsymbol{\varphi}_{h\tau})_{\Omega^b} + a_h^b(\boldsymbol{u}_{h\tau},\boldsymbol{\varphi}_{h\tau}) \\
& + J_h^b(\boldsymbol{u}_{h\tau},\boldsymbol{\varphi}_{h\tau})\Big)\,\mathrm{d}t + (\{\boldsymbol{y}_{h\tau}\}_{m-1},\boldsymbol{\varphi}_{h\tau}(t_{m-1}+))_{\Omega^b} \\
= {} & \int_{I_m} l_h^b(\boldsymbol{\varphi}_{h\tau})\,\mathrm{d}t \quad \forall\,\boldsymbol{\varphi}_{h\tau}\in\boldsymbol{S}_{h\tau}^{b,sq^*},
\end{aligned} \tag{3.29}
$$

$$
\begin{aligned}
\int_{I_m}\Big(\Big(\frac{\partial\boldsymbol{u}_{h\tau}}{\partial t},\boldsymbol{\varphi}_{h\tau}\Big)_{\Omega^b} - (\boldsymbol{y}_{h\tau},\boldsymbol{\varphi}_{h\tau})_{\Omega^b}\Big)\,\mathrm{d}t & \\
+ (\{\boldsymbol{u}_{h\tau}\}_{m-1},\boldsymbol{\varphi}_{h\tau}(t_{m-1}+))_{\Omega^b} = 0 \quad \forall\,\boldsymbol{\varphi}_{h\tau}\in\boldsymbol{S}_{h\tau}^{b,sq^*},\ m=1,\dots,M. &
\end{aligned} \tag{3.30}
$$

Similarly to (3.16) we define the initial states $\boldsymbol{u}_h(0-)$, $\boldsymbol{y}_h(0-)\in\boldsymbol{S}_h^{b,s}$ by

$$
\begin{aligned}
(\boldsymbol{u}_h(0-),\boldsymbol{\varphi}_h)_{\Omega^b} &= (\boldsymbol{u}^0,\boldsymbol{\varphi}_h)_{\Omega^b} \quad \forall\,\boldsymbol{\varphi}_h\in\boldsymbol{S}_h^{b,s}, \\
(\boldsymbol{y}_h(0-),\boldsymbol{\varphi}_h)_{\Omega^b} &= (\boldsymbol{y}^0,\boldsymbol{\varphi}_h)_{\Omega^b} \quad \forall\,\boldsymbol{\varphi}_h\in\boldsymbol{S}_h^{b,s}.
\end{aligned} \tag{3.31}
$$

3.3. Coupling procedure. In the solution of the complete coupled FSI problem it is necessary to apply a suitable coupling procedure. See, e.g., [2] for a general framework. Here we apply the following algorithm, in which we proceed successively from one time interval $[t_k, t_{k+1}]$ to the next interval $[t_{k+1}, t_{k+2}]$.

(1) Assume that the approximate solution of the flow problem on the time level t_k as well as the deformation of the structure $\boldsymbol{u}_{h\tau,k}$ are known.

(2) Set $\boldsymbol{u}^0_{h\tau,k+1} := \boldsymbol{u}_{h\tau,k}$, $l := 1$, and apply the iterative process:

   (a) Compute the stress tensor $\boldsymbol{\tau}^f$ and the aerodynamical force acting on the structure and transform it to the interface Γ^b_N.

   (b) Solve the elasticity problem, compute the deformation $\boldsymbol{u}^l_{h\tau,k+1}$ at time t_{k+1} and approximate the flow domain $\Omega^l_{t_{k+1}}$.

   (c) Determine the ALE mapping $\mathcal{A}^l_{t_{k+1}h}$ and approximate the domain velocity $\boldsymbol{z}^l_{h,k+1}$.

   (d) Solve the flow problem on the approximation of $\Omega^l_{t_{k+1}}$.

   (e) If the variation of the displacement $|\boldsymbol{u}^l_{h\tau,k+1} - \boldsymbol{u}^{l-1}_{h\tau,k+1}|$ is larger than the prescribed tolerance, then set $l := l + 1$ and go to (a). Else $k := k + 1$ and go to (2).

This algorithm represents the so-called strong coupling. If in the step (e) we set $k := k + 1$ and go to (2) already in the case when $l = 1$, then we get the weak (loose) coupling.

4. Algorithmization and numerical realization of the coupled problem

The linear algebraic systems equivalent to (3.16) and (3.18) are solved either by the direct solver UMFPACK ([14]) or by the GMRES method with block diagonal preconditioning. These methods are also used for the solution of the structure problem (3.29)–(3.31). In the case of nonlinear elasticity on each time level the nonlinear system is solved by the Newton method.

4.1. Newton method. In the case of nonlinear elasticity model, the form $a^b_h(\boldsymbol{u}, \boldsymbol{\varphi})$ is linear with respect to $\boldsymbol{\varphi}$, but nonlinear in $\boldsymbol{u}$. As a consequence, the STDGM discrete scheme results in systems of nonlinear algebraic equations. For their solution we apply the Newton method (see [15]), which was applied in, e.g., [30] and [35], where the incompressible flow model and the conforming finite element discretization were employed.

Let $\boldsymbol{f}\colon \mathbb{R}^N \to \mathbb{R}^N$. We seek a solution $\boldsymbol{\alpha} \in \mathbb{R}^N$ such that $\boldsymbol{f}(\boldsymbol{\alpha}) = 0$. The Newton algorithm to obtain a solution is the following: let $\boldsymbol{\alpha}^{(0)}$ be an initial guess of the sought solution and let $\varepsilon > 0$ be a given tolerance. For $i \geqslant 0$ iterate:

(1) Evaluate the residual $\boldsymbol{r}^{(i)} = \boldsymbol{f}(\boldsymbol{\alpha}^{(i)})$.
(2) Check the residual and stop iterations with $\boldsymbol{\alpha} := \boldsymbol{\alpha}^{(i)}$ if $\|\boldsymbol{r}^{(i)}\| \leqslant \varepsilon$.
(3) Compute $\delta\boldsymbol{\alpha}$ from

$$\nabla_{\boldsymbol{\alpha}} \boldsymbol{f}(\boldsymbol{\alpha}^{(i)})\delta\boldsymbol{\alpha} = \boldsymbol{r}^{(i)}. \tag{4.1}$$

(4) Update $\boldsymbol{\alpha}^{(i+1)} := \boldsymbol{\alpha}^{(i)} - \delta\boldsymbol{\alpha}$, set $i := i + 1$ and go to 1.

Note that (4.1) represents a system of linear algebraic equations.

4.2. Realization of the discrete elasticity problem. We shall now briefly discuss the application of the Newton method to our discretization of the nonlinear elasticity problem. We can express the sought approximate solution as a linear combination of basis functions in the space $[\mathcal{V}]^2$.

Let ψ_i, $i = 1, \ldots, N = \dim \mathcal{V}$, be a basis of $\mathcal{V}$. Then the sought solution $\boldsymbol{u}_{h\tau}$ can be expressed as

$$\boldsymbol{u}_{h\tau} = \boldsymbol{u}_{h\tau}(\boldsymbol{\alpha}) = \sum_{i=1}^{2N} \alpha_i \boldsymbol{\phi}_i, \tag{4.2}$$

where $\boldsymbol{\alpha} = (\alpha_i)_{i=1}^{2N}$ are the finite element coefficients and where $\boldsymbol{\phi}_i = (\psi_i, 0)$ for $1 \leqslant i \leqslant N$ and $\boldsymbol{\phi}_i = (0, \psi_{i-N})$ for $N < i \leqslant 2N$ form the basis of $[\mathcal{V}]^2$.

In order to apply the Newton method as defined in Subsection 4.1, we must differentiate the form $a_h^b(\boldsymbol{u}_{h\tau}(\boldsymbol{\alpha}), \boldsymbol{\varphi})$ (and subsequently the tensor $\boldsymbol{P}$) with respect to the coefficients $\boldsymbol{\alpha}$. For clarity, we shall denote the gradient with respect to $\boldsymbol{\alpha}$ by $\nabla_{\boldsymbol{\alpha}}$ and the gradient with respect to $\boldsymbol{X} = (x_1, x_2) \in \Omega_b$ by $\nabla_{\boldsymbol{X}}$. Clearly

$$\begin{aligned} &\frac{\partial}{\partial\alpha_k}\boldsymbol{u}_{h\tau} = (\psi_i, 0), \quad 1 \leqslant k \leqslant N,\ i = k, \\ &\frac{\partial}{\partial\alpha_k}\boldsymbol{u}_{h\tau} = (0, \psi_i), \quad N < k \leqslant 2N,\ i = k - N, \end{aligned} \tag{4.3}$$

and

$$\begin{aligned} \nabla_{\boldsymbol{X}}\boldsymbol{u}_{h\tau} &= \sum_{i=1}^{N} \alpha_i \nabla_{\boldsymbol{X}}(\psi_i, 0) + \sum_{i=1}^{N} \alpha_{i+N} \nabla_{\boldsymbol{X}}(0, \psi_i) \\ &= \begin{pmatrix} \sum\limits_{i=1}^{N} \alpha_i \dfrac{\partial\psi_i}{\partial x_1}, & \sum\limits_{i=1}^{N} \alpha_i \dfrac{\partial\psi_i}{\partial x_2} \\ \sum\limits_{i=1}^{N} \alpha_{i+N} \dfrac{\partial\psi_i}{\partial x_1}, & \sum\limits_{i=1}^{N} \alpha_{i+N} \dfrac{\partial\psi_i}{\partial x_2} \end{pmatrix}. \end{aligned} \tag{4.4}$$

By (2.12) and (2.13),

$$\boldsymbol{P}(\boldsymbol{F}) = \boldsymbol{P}(\nabla_{\boldsymbol{X}}\boldsymbol{X} + \nabla_{\boldsymbol{X}}\boldsymbol{u}). \tag{4.5}$$

Taking into account that $\nabla_{\boldsymbol{X}}(\boldsymbol{X})$ is the constant unit matrix $\mathbb{I}$, we introduce the simplified notation

$$\widetilde{\boldsymbol{P}}(\nabla_{\boldsymbol{X}}\mathbf{u}) = \boldsymbol{P}(\mathbb{I} + \nabla_{\boldsymbol{X}}\boldsymbol{u}). \tag{4.6}$$

Now the gradient of the form a_h^b can be expressed as

$$\begin{aligned}\nabla_{\boldsymbol{\alpha}} a_h^b(\boldsymbol{u}_{h\tau}(\boldsymbol{\alpha}), \boldsymbol{\varphi}) = {} & \sum_{K\in\mathcal{T}_h{}^b} \int_K \nabla_{\boldsymbol{\alpha}}(\widetilde{\boldsymbol{P}}(\nabla_{\boldsymbol{X}}\boldsymbol{u}_{h\tau}(\boldsymbol{\alpha})) : \nabla_{\boldsymbol{X}}\boldsymbol{\varphi})\,\mathrm{d}\boldsymbol{x} \\ & - \sum_{\Gamma\in\mathcal{F}_h^{b,I}\cup\mathcal{F}_h^{b,D}} \int_\Gamma \nabla_{\boldsymbol{\alpha}}(\langle\widetilde{\boldsymbol{P}}(\nabla_{\boldsymbol{X}}\boldsymbol{u}_{h\tau}(\boldsymbol{\alpha}))\rangle\boldsymbol{n}\cdot[\boldsymbol{\varphi}])\,\mathrm{d}S \\ & + \sum_{\Gamma\in\mathcal{F}_h^{b,I}\cup\mathcal{F}_h^{b,D}} \int_\Gamma \frac{C_W^b}{h_\Gamma}\nabla_{\boldsymbol{\alpha}}([\boldsymbol{u}_{h\tau}(\boldsymbol{\alpha})]\cdot[\boldsymbol{\varphi}])\,\mathrm{d}S.\end{aligned} \tag{4.7}$$

Let $\widetilde{\boldsymbol{P}}(\nabla_{\boldsymbol{X}}\boldsymbol{u}_{h\tau}(\boldsymbol{\alpha})) = (P_{ij})_{i,j=1}^2$ (here for simplicity we do not explicitly write the dependence of P_{ij} on $\nabla_{\boldsymbol{X}}\boldsymbol{u}_{h\tau}(\boldsymbol{\alpha})$) and let $\boldsymbol{\varphi} = (\varphi_1, \varphi_2)$. From

$$\widetilde{\boldsymbol{P}}(\nabla_{\boldsymbol{X}}\boldsymbol{u}_{h\tau}(\boldsymbol{\alpha})) : \nabla_{\boldsymbol{X}}\boldsymbol{\varphi} = P_{11}\frac{\partial\varphi_1}{\partial x_1} + P_{12}\frac{\partial\varphi_1}{\partial x_2} + P_{21}\frac{\partial\varphi_2}{\partial x_1} + P_{22}\frac{\partial\varphi_2}{\partial x_2}, \tag{4.8}$$

we obtain that

$$\begin{aligned}\frac{\partial}{\partial\alpha_k}(\widetilde{\boldsymbol{P}}(\nabla_{\boldsymbol{X}}\boldsymbol{u}_{h\tau}(\boldsymbol{\alpha})) : \nabla_{\boldsymbol{X}}\boldsymbol{\varphi}) = {} & \frac{\partial}{\partial\alpha_k}P_{11}\frac{\partial\varphi_1}{\partial x_1} + \frac{\partial}{\partial\alpha_k}P_{12}\frac{\partial\varphi_1}{\partial x_2} \\ & + \frac{\partial}{\partial\alpha_k}P_{21}\frac{\partial\varphi_2}{\partial x_1} + \frac{\partial}{\partial\alpha_k}P_{22}\frac{\partial\varphi_2}{\partial x_2}, \\ \frac{\partial}{\partial\alpha_k}(\langle\widetilde{\boldsymbol{P}}(\nabla_{\boldsymbol{X}}\boldsymbol{u}_{h\tau}(\boldsymbol{\alpha}))\rangle\boldsymbol{n}\cdot[\boldsymbol{\varphi}]) = {} & \Big(\frac{\partial}{\partial\alpha_k}\langle P_{11}\rangle n_1 + \frac{\partial}{\partial\alpha_k}\langle P_{12}\rangle n_2\Big)[\varphi_1] \\ & + \Big(\frac{\partial}{\partial\alpha_k}\langle P_{21}\rangle n_1 + \frac{\partial}{\partial\alpha_k}\langle P_{22}\rangle n_2\Big)[\varphi_2].\end{aligned} \tag{4.9}$$

Now for $\boldsymbol{\varphi} = (\psi_j, 0)$ we have

$$\widetilde{\boldsymbol{P}}(\nabla_{\boldsymbol{X}}\boldsymbol{u}_{h\tau}(\boldsymbol{\alpha})) : \nabla_{\boldsymbol{X}}\boldsymbol{\varphi} = P_{11}\frac{\partial\psi_j}{\partial x_1} + P_{12}\frac{\partial\psi_j}{\partial x_2}, \tag{4.10}$$

$$\frac{\partial}{\partial\alpha_k}(\widetilde{\boldsymbol{P}}(\nabla_{\boldsymbol{X}}\boldsymbol{u}_{h\tau}(\boldsymbol{\alpha})) : \nabla_{\boldsymbol{X}}\boldsymbol{\varphi}) = \frac{\partial}{\partial\alpha_k}P_{11}\frac{\partial\psi_j}{\partial x_1} + \frac{\partial}{\partial\alpha_k}P_{12}\frac{\partial\psi_j}{\partial x_2}, \tag{4.11}$$

$$\frac{\partial}{\partial\alpha_k}(\langle\widetilde{\boldsymbol{P}}(\nabla_{\boldsymbol{X}}\boldsymbol{u}_{h\tau}(\boldsymbol{\alpha}))\rangle\boldsymbol{n}\cdot[\boldsymbol{\varphi}]) = \Big(\frac{\partial}{\partial\alpha_k}\langle P_{11}\rangle n_1 + \frac{\partial}{\partial\alpha_k}\langle P_{12}\rangle n_2\Big)[\psi_j], \tag{4.12}$$

while for $\boldsymbol{\varphi} = (0, \psi_j)$ we have

$$\widetilde{\boldsymbol{P}}(\nabla_{\boldsymbol{X}} \boldsymbol{u}_{h\tau}(\boldsymbol{\alpha})) : \nabla_{\boldsymbol{X}} \boldsymbol{\varphi} = P_{21} \frac{\partial \psi_j}{\partial x_1} + P_{22} \frac{\partial \psi_j}{\partial x_2}, \tag{4.13}$$

$$\frac{\partial}{\partial \alpha_k} (\widetilde{\boldsymbol{P}}(\nabla_{\boldsymbol{X}} \boldsymbol{u}_{h\tau}(\boldsymbol{\alpha})) : \nabla_{\boldsymbol{X}} \boldsymbol{\varphi}) = \frac{\partial}{\partial \alpha_k} P_{21} \frac{\partial \psi_j}{\partial x_1} + \frac{\partial}{\partial \alpha_k} P_{22} \frac{\partial \psi_j}{\partial x_2}, \tag{4.14}$$

$$\frac{\partial}{\partial \alpha_k} (\langle \widetilde{\boldsymbol{P}}(\nabla_{\boldsymbol{X}} \boldsymbol{u}_{h\tau}(\boldsymbol{\alpha})) \rangle \boldsymbol{n} \cdot [\boldsymbol{\varphi}]) = \Big(\frac{\partial}{\partial \alpha_k} \langle P_{21} \rangle n_1 + \frac{\partial}{\partial \alpha_k} \langle P_{22} \rangle n_2 \Big) [\psi_j]. \tag{4.15}$$

It remains to express the derivatives of the tensor $\widetilde{\boldsymbol{P}}$—for our choice of the neo-Hookean material they can be found in Section 4.3.

The Newton method is applied at each time step for the solution of the nonlinear discrete problem. Each iteration of the Newton method represents a linear algebraic system and is solved by the direct solver UMFPACK (cf. [14]).

4.3. Neo-Hookean material—derivatives. Let $\widetilde{\boldsymbol{P}} = \widetilde{\boldsymbol{P}}(\boldsymbol{u}_{h\tau}(\boldsymbol{\alpha})) = (P_{ij})_{i,j=1}^2$ be the first Piola-Kirchhoff tensor of the neo-Hookean material as defined in (2.22). Let $\boldsymbol{u}_{h\tau}(\boldsymbol{\alpha}) = (u_1, u_2)$. From (2.13) and (2.22) we get

$$P_{11} = \mu^b \Big(1 + \frac{\partial u_1}{\partial x_1} \Big) + c_1 \Big(1 + \frac{\partial u_2}{\partial x_2} \Big), \tag{4.16}$$

$$P_{12} = \mu^b \frac{\partial u_1}{\partial x_2} - c_1 \frac{\partial u_2}{\partial x_1}, \tag{4.17}$$

$$P_{21} = \mu^b \frac{\partial u_2}{\partial x_1} - c_1 \frac{\partial u_1}{\partial x_2}, \tag{4.18}$$

$$P_{22} = \mu^b \Big(1 + \frac{\partial u_2}{\partial x_2} \Big) + c_1 \Big(1 + \frac{\partial u_1}{\partial x_1} \Big), \tag{4.19}$$

where

$$c_1 = \frac{\lambda^b \log(\det \boldsymbol{F}) - \mu^b}{\det \boldsymbol{F}}. \tag{4.20}$$

Now let $\boldsymbol{u}_{h\tau}(\boldsymbol{\alpha}) = (u_1, u_2) = \sum\limits_{k=1}^{2N} \alpha_k \boldsymbol{\psi}_k$, where $\boldsymbol{\psi}_k = (\psi_k, 0)$ for $1 \leqslant k \leqslant N$ and $\boldsymbol{\psi}_k = (0, \psi_{k-N})$ for $N < k \leqslant 2N$.

Let us express first the derivative of the determinant of $\boldsymbol{F}$ with respect to the coefficient α_k. If $1 \leqslant k \leqslant N$ and $i := k$, then

$$\frac{\partial}{\partial \alpha_k} (\det \boldsymbol{F}) = \frac{\partial \psi_i}{\partial x_1} \Big(\frac{\partial u_2}{\partial x_2} + 1 \Big) - \frac{\partial \psi_i}{\partial x_2} \frac{\partial u_2}{\partial x_1}, \tag{4.21}$$

and for $N < k \leqslant 2N$, $i := k - N$:

$$\frac{\partial}{\partial \alpha_k} (\det \boldsymbol{F}) = \frac{\partial \psi_i}{\partial x_2} \Big(\frac{\partial u_1}{\partial x_1} + 1 \Big) - \frac{\partial \psi_i}{\partial x_1} \frac{\partial u_1}{\partial x_2}. \tag{4.22}$$

The derivatives of $\widetilde{\boldsymbol{P}}(\boldsymbol{u}_{h\tau}(\boldsymbol{\alpha}))$ with respect to the coefficient α_k are given as follows: If $1 \leqslant k \leqslant N$ and $i := k$, then

$$\frac{\partial}{\partial\alpha_k}P_{11} = \mu^b\frac{\partial\psi_i}{\partial x_1} + c_2\frac{\partial}{\partial\alpha_k}(\det\boldsymbol{F})\Big(1+\frac{\partial u_2}{\partial x_2}\Big), \tag{4.23}$$

$$\frac{\partial}{\partial\alpha_k}P_{12} = \mu^b\frac{\partial\psi_i}{\partial x_2} - c_2\frac{\partial}{\partial\alpha_k}(\det\boldsymbol{F})\frac{\partial u_2}{\partial x_1}, \tag{4.24}$$

$$\frac{\partial}{\partial\alpha_k}P_{21} = -c_1\frac{\partial\psi_i}{\partial x_2} - c_2\frac{\partial}{\partial\alpha_k}(\det\boldsymbol{F})\frac{\partial u_1}{\partial x_2}, \tag{4.25}$$

$$\frac{\partial}{\partial\alpha_k}P_{22} = c_1\frac{\partial\psi_i}{\partial x_1} + c_2\frac{\partial}{\partial\alpha_k}(\det\boldsymbol{F})\Big(1+\frac{\partial u_1}{\partial x_1}\Big), \tag{4.26}$$

where c_1 is as in (4.20),

$$c_2 = \frac{\lambda^b - \lambda^b\log(\det\boldsymbol{F}) + \mu^b}{(\det\boldsymbol{F})^2}, \tag{4.27}$$

and $\frac{\partial}{\partial\alpha_k}(\det\boldsymbol{F})$ is expressed in (4.21).

Finally, for $N < k \leqslant 2N$ we set $i = k - N$ and get

$$\frac{\partial}{\partial\alpha_k}P_{11} = c_1\frac{\partial\psi_i}{\partial x_2} + c_2\frac{\partial}{\partial\alpha_k}(\det\boldsymbol{F})\Big(1+\frac{\partial u_2}{\partial x_2}\Big), \tag{4.28}$$

$$\frac{\partial}{\partial\alpha_k}P_{12} = -c_1\frac{\partial\psi_i}{\partial x_1} - c_2\frac{\partial}{\partial\alpha_k}(\det\boldsymbol{F})\frac{\partial u_2}{\partial x_1}, \tag{4.29}$$

$$\frac{\partial}{\partial\alpha_k}P_{21} = \mu^b\frac{\partial\psi_i}{\partial x_1} - c_2\frac{\partial}{\partial\alpha_k}(\det\boldsymbol{F})\frac{\partial u_1}{\partial x_2}, \tag{4.30}$$

$$\frac{\partial}{\partial\alpha_k}P_{22} = \mu^b\frac{\partial\psi_i}{\partial x_2} + c_2\frac{\partial}{\partial\alpha_k}(\det\boldsymbol{F})\Big(1+\frac{\partial u_1}{\partial x_1}\Big), \tag{4.31}$$

where c_1 is as in (4.20), c_2 as in (4.27) and $\frac{\partial}{\partial\alpha_k}(\det\boldsymbol{F})$ is expressed in (4.22).

5. Numerical experiments

Now we present our numerical results for a simplified vocal folds model. The geometry of the domain occupied by the fluid and its size are given in Figure 1. Moreover, we add to this geometry a semicircle subdomain with a radius 3.0 cm as an outlet Γ_O.

We prescribe the inlet boundary conditions on Γ_I (left part of the boundary), the outlet boundary conditions on Γ_O (right part of the boundary, which is a semicircle), and we prescribe boundary conditions on the impermeable fixed walls Γ_W (including the vertical segments of the semicircle) and on the moving impermeable walls denoted

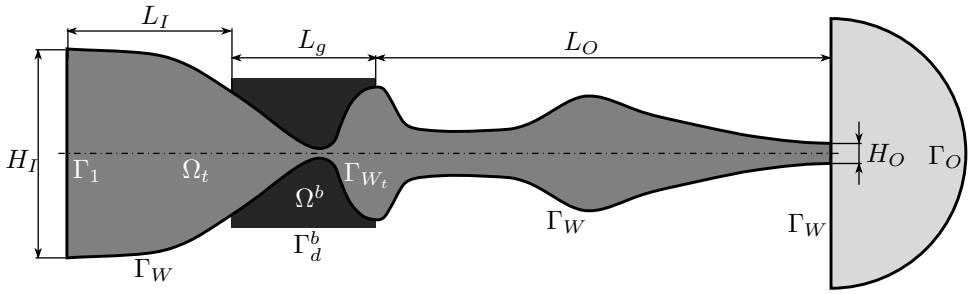

Figure 1. Geometry of the computational domain at time $t = 0$ and the description of its size: $L_I = 20.0$ mm, $L_g = 17.5$ mm, $L_O = 55.0$ mm, $H_I = 25.5$ mm, $H_O = 2.76$ mm.

in Figure 1 by Γ_{W_t}. The fluid flow problem is computed on the triangulation with 17652 elements. Further, for the definition of the fluid flow problem the following data are used:

magnitude of the inlet velocity	$v_{\text{in}} = 4\,\text{m}\,\text{s}^{-1}$,
dynamic viscosity	$\mu = 1.80 \cdot 10^{-5}\,\text{kg}\,\text{m}^{-1}s^{-1}$,
inlet density	$\varrho_{\text{in}} = 1.225\,\text{kg}\,\text{m}^{-3}$,
outlet pressure	$p_{\text{out}} = 97611\,\text{Pa}$,
Reynolds number	$\text{Re} = \varrho_{\text{in}} v_{\text{in}} H_I/\mu = 6941.7$,
heat conduction coefficient	$\kappa = 2.428 \cdot 10^{-2}\,\text{kg}\,\text{m}\,\text{s}^{-3}\,\text{K}^{-1}$,
specific heat	$c_v = 721.428\,\text{m}^2\,\text{s}^{-2}\,\text{K}^{-1}$,
Poisson adiabatic constant	$\gamma = 1.4$.

For the fluid solver we use the STDGM with polynomial approximation of degree 2 in space and degree 1 in time. We employ the IIPG version of the DGM with the penalization constant $C_W = 500$ for inner faces and $C_W = 5000$ for boundary edges. The stabilization parameters ν_1 and ν_2 from (3.13) are set to 0.1. The time step τ is set to $1.0 \cdot 10^{-6}$ s. For the first 1000 time steps the fluid flow is computed with the fixed boundary. Then the part Γ_{W_t} of the boundary is released and we solve the FSI problem.

We assume that the elastic bodies resulting from a cut of vocal folds are isotropic with constant material density $\varrho^b = 1040\ \text{kg}\,\text{m}^{-3}$. The triangulation used for the solution of the structure problem has 5118 elements, see Figure 2. The division of the domain into 4 regions with different material characteristics is illustrated in Figure 3 by the Lamé parameters and the setting of the material characteristics is described in Table 1.

Further, the initial displacement and the initial deformation velocity are set to be zero. On the bottom, right and left straight parts of the boundary we prescribe

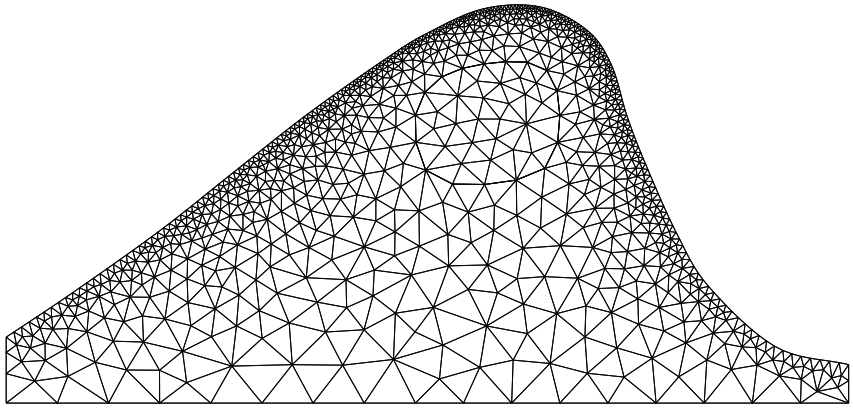

Figure 2. Model of vocal folds—computational mesh.

E^b	ν^b	λ^b	μ^b
$12 \cdot 10^3$	0.4	17143	4285
$8 \cdot 10^3$	0.4	11430	2857
$1 \cdot 10^3$	0.495	33110	335
$100 \cdot 10^3$	0.4	142857	35714

Table 1. Nonhomogeneous model of vocal folds—Lamé parameters. See Figure 3 for the visualization of the corresponding subdomains, ordered from the lower layer to the upper layer.

homogeneous Dirichlet boundary condition (2.15) and on the curved part of the boundary the Neumann boundary condition (2.16). The damping coefficient c_M is set to 1.0 s^{-1}. For the solution of the dynamic elasticity problem we employ the NIPG version of the DGM, where the penalization constant is set to $C_W^b = 4 \cdot 10^6$.

The ALE mapping is determined as described in Section 2.4. For the solution of the static elasticity problem (2.26) we employ the NIPG version of the DGM, where the penalization constant is set to $C_W = 10^3$. Then the DG solution of the ALE discrete problem (2.26) is interpolated to a continuous approximation.

We use the strong coupling algorithm described in Section 3.3 with the prescribed tolerance 10^{-5}. Further, we use 5 coupling subiterations as the maximum, however the prescribed tolerance was usually reached after 2–3 coupling subiterations.

In what follows we compare the linear strain tensor $\boldsymbol{e}$ and the nonlinear Green strain tensor $\boldsymbol{E} \in \mathbb{R}^{2\times 2}$, see [13], defined by

$$\boldsymbol{E} = \frac{1}{2}(\boldsymbol{F}^\top \boldsymbol{F} - \mathbb{I}), \quad \boldsymbol{E} = (E_{ij})_{i,j=1}^2 \tag{5.1}$$

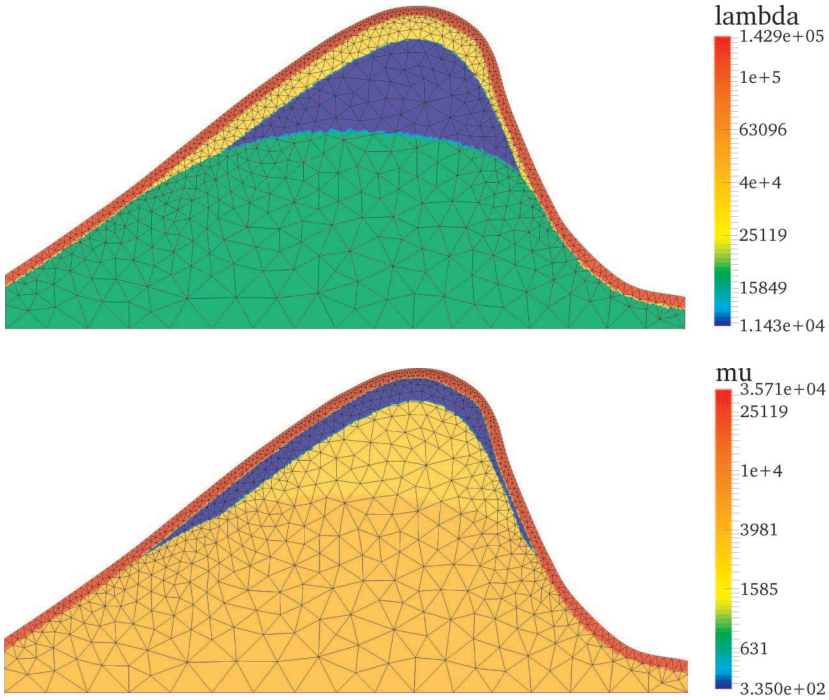

Figure 3. Nonhomogeneous model of vocal folds—Lamé parameters.

with components

$$E_{ij} = \underbrace{\frac{1}{2}\Big(\frac{\partial u_i}{\partial x_j} + \frac{\partial u_j}{\partial x_i}\Big)}_{e_{ij}\text{-linear part}} + \underbrace{\frac{1}{2}\sum_{k=1}^{2}\frac{\partial u_k}{\partial x_i}\frac{\partial u_k}{\partial x_j}}_{E^*_{ij}\text{-nonlinear part}}. \tag{5.2}$$

In the case of the linear elasticity the stress tensor depends on the strain tensor $\boldsymbol{e} = (e_{ij})_{i,j=1}^2$ and in the case of nonlinear elasticity it depends on $\boldsymbol{E} = \boldsymbol{e} + \boldsymbol{E}^*$, where $\boldsymbol{E}^* = (E^*_{ij})_{i,j=1}^2$.

The influence of the nonlinear part of the strain tensor is given by the ratio

$$R := \frac{\|\boldsymbol{e}\|}{\|\boldsymbol{E}\|} = \frac{\|\boldsymbol{e}\|}{\|\boldsymbol{e} + \boldsymbol{E}^*\|}. \tag{5.3}$$

If $R \approx 1$, then the nonlinear part of the strain tensor has no influence on the computation (the linear elasticity model is sufficient), but if $R \approx 0$, then the nonlinear part strongly takes effect and it is necessary to use a nonlinear elasticity model. Figure 4 shows numerical simulation of the vocal folds from the beginning of the FSI computation at 12 time instants. Figure 5 shows in detail the deformation of

the vocal folds at 2 time instants for a maximal and minimal glottal gap during vocal folds oscillations. In Figures 4 and 5 the case $R \approx 1$ is depicted by white and the case $R \approx 0$ by dark red color. It can be seen that the nonlinear part of the strain tensor takes effect in elements near to the boundary, therefore to correctly capture the deformations of the vocal folds, it is necessary to use a nonlinear model of elasticity.

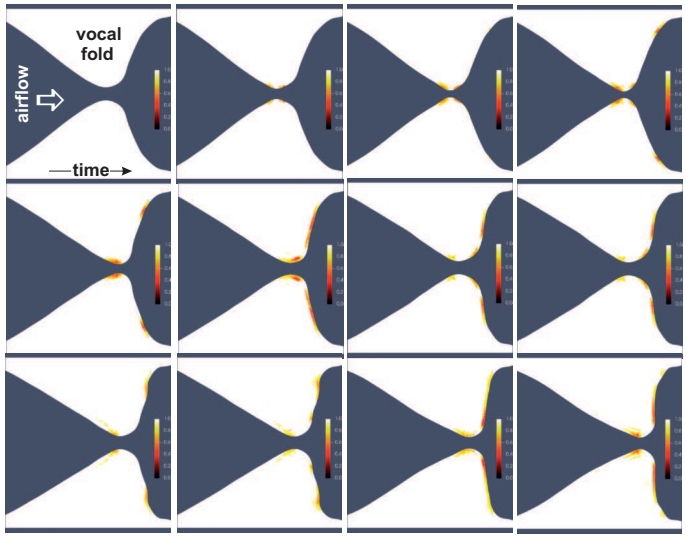

Figure 4. Deformation of vocal folds in dependence on time and the ratios of the norms of the linear strain tensor and the nonlinear Green strain tensor at different time instants.

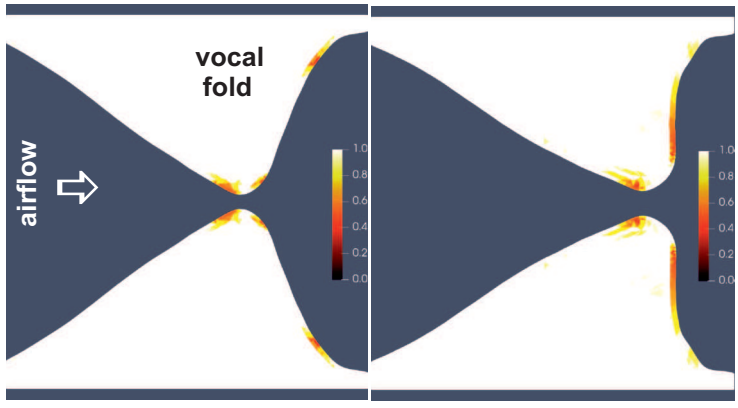

Figure 5. Deformation of vocal folds in dependence on time and the ratios of the norms of the linear strain tensor and the nonlinear Green strain tensor at different time instants—details for the smallest and the largest glottal gap between the vocal folds.

6. Conclusion

The paper shows the applicability of the space-time discontinuous Galerkin method in time dependent domains in the case of a fluid-structure interaction problem. We present a detailed description of this method used both for the solution of compressible Navier-Stokes equations written in the ALE form and for the solution of nonlinear elasticity problem using the neo-Hookean model. The method which we worked out is applied to the numerical simulation of vocal folds vibrations caused by the air flow in the vocal tract model. The shape and material properties of the elastic bodies are motivated by human vocal folds. The method allows us to assume that the elastic body is formed by several parts with different material characteristics. The novelty of the paper is the exemplification that the STDGM is suitable for numerical solution of fluid structure interaction, especially to the simulation of vocal folds vibrations. An important result is the demonstration that for the simulation of vocal folds vibrations it is necessary to use the model of nonlinear elasticity, because the linear elasticity model is not adequate.

Future work should be concentrated on the realization of a remeshing in the case of closing the glottal channel during the oscillation period of the channel walls and the identification of the acoustic signal.

References

[1] *G. Akrivis, C. Makridakis*: Galerkin time-stepping methods for nonlinear parabolic equations. M2AN, Math. Model. Numer. Anal. *38* (2004), 261–289. zbl MR doi

[2] *S. Badia, R. Codina*: On some fluid-structure iterative algorithms using pressure segregation methods. Application to aeroelasticity. Int. J. Numer. Methods Eng. *72* (2007), 46–71. zbl MR doi

[3] *M. Balázsová, M. Feistauer*: On the stability of the ALE space-time discontinuous Galerkin method for nonlinear convection-diffusion problems in time-dependent domains. Appl. Math., Praha *60* (2015), 501–526. zbl MR doi

[4] *M. Balázsová, M. Feistauer, M. Hadrava, A. Kosík*: On the stability of the space-time discontinuous Galerkin method for the numerical solution of nonstationary nonlinear convection-diffusion problems. J. Numer. Math. *23* (2015), 211–233. zbl MR doi

[5] *D. Boffi, L. Gastaldi, L. Heltai*: Numerical stability of the finite element immersed boundary method. Math. Models Methods Appl. Sci. *17* (2007), 1479–1505. zbl MR doi

[6] *J. Bonet, R. D. Wood*: Nonlinear Continuum Mechanics for Finite Element Analysis. Cambridge University Press, Cambridge, 2008. zbl MR doi

[7] *A. Bonito, I. Kyza, R. H. Nochetto*: Time-discrete higher-order ALE formulations: stability. SIAM J. Numer. Anal. *51* (2013), 577–604. zbl MR doi

[8] *J. Česenek, M. Feistauer*: Theory of the space-time discontinuous Galerkin method for nonstationary parabolic problems with nonlinear convection and diffusion. SIAM J. Numer. Anal. *50* (2012), 1181–1206. zbl MR doi

[9] *J. Česenek, M. Feistauer, J. Horáček, V. Kučera, J. Prokopová*: Simulation of compressible viscous flow in time-dependent domains. Appl. Math. Comput. *219* (2013), 7139–7150. zbl MR doi

[10] *J. Česenek, M. Feistauer, A. Kosík*: DGFEM for the analysis of airfoil vibrations induced by compressible flow. ZAMM, Z. Angew. Math. Mech. *93* (2013), 387–402. zbl MR doi
[11] *K. Chrysafinos, N. J. Walkington*: Error estimates for the discontinuous Galerkin methods for parabolic equations. SIAM J. Numer. Anal. *44* (2006), 349–366. zbl MR doi
[12] *P. G. Ciarlet*: The Finite Element Method for Elliptic Problems. Studies in Mathematics and Its Applications 4, North-Holland Publishing Company, Amsterdam, 1978. zbl MR doi
[13] *P. G. Ciarlet*: Mathematical Elasticity. Volume I: Three-Dimensional Elasticity. Studies in Mathematics and Its Applications 20, North-Holland, Amsterdam, 1988. zbl MR doi
[14] *T. A. Davis, I. S. Duff*: A combined unifrontal/multifrontal method for unsymmetric sparse matrices. ACM Trans. Math. Softw. *25* (1999), 1–20. zbl MR doi
[15] *P. Deuflhard*: Newton Methods for Nonlinear Problems. Affine Invariance and Adaptive Algorithms. Springer Series in Computational Mathematics 35, Springer, Berlin, 2004. zbl MR doi
[16] *V. Dolejší, M. Feistauer*: Discontinuous Galerkin Method. Analysis and Applications to Compressible Flow. Springer Series in Computational Mathematics 48, Springer, Cham, 2015. zbl MR doi
[17] *V. Dolejší, M. Feistauer, C. Schwab*: On some aspects of the discontinuous Galerkin finite element method for conservation laws. Math. Comput. Simul. *61* (2003), 333–346. zbl MR doi
[18] *J. Donea, S. Giuliani, J. P. Halleux*: An arbitrary Lagrangian-Eulerian finite element method for transient dynamic fluid-structure interactions. Comput. Methods Appl. Mech. Eng. *33* (1982), 689–723. zbl doi
[19] *K. Eriksson, D. Estep, P. Hansbo, C. Johnson*: Computational Differential Equations. Cambridge University Press, Cambridge, 1996. zbl MR
[20] *K. Eriksson, C. Johnson*: Adaptive finite element methods for parabolic problems. I. A linear model problem. SIAM J. Numer. Anal. *28* (1991), 43–77. zbl MR doi
[21] *D. Estep, S. Larsson*: The discontinuous Galerkin method for semilinear parabolic problems. RAIRO, Modélisation Math. Anal. Numér. *27* (1993), 35–54. zbl MR doi
[22] *M. Feistauer, J. Česenek, J. Horáček, V. Kučera, J. Prokopová*: DGFEM for the numerical solution of compressible flow in time dependent domains and applications to fluid-structure interaction. Proceedings of the 5th European Conference on Computational Fluid Dynamics ECCOMAS CFD 2010 (J. C. F. Pereira, A. Sequeira, eds.). Lisbon, Portugal (published ellectronically), 2010.
[23] *M. Feistauer, J. Felcman, I. Straškraba*: Mathematical and Computational Methods for Compressible Flow. Numerical Mathematics and Scientific Computation, Oxford University Press, Oxford, 2003. zbl MR
[24] *M. Feistauer, J. Hájek, K. Švadlenka*: Space-time discontinuous Galerkin method for solving nonstationary convection-diffusion-reaction problems. Appl. Math., Praha *52* (2007), 197–233. zbl MR doi
[25] *M. Feistauer, J. Hasnedlová-Prokopová, J. Horáček, A. Kosík, V. Kučera*: DGFEM for dynamical systems describing interaction of compressible fluid and structures. J. Comput. Appl. Math. *254* (2013), 17–30. zbl MR doi
[26] *M. Feistauer, J. Horáček, V. Kučera, J. Prokopová*: On numerical solution of compressible flow in time-dependent domains. Math. Bohem. *137* (2012), 1–16. zbl MR
[27] *M. Feistauer, V. Kučera*: On a robust discontinuous Galerkin technique for the solution of compressible flow. J. Comput. Phys. *224* (2007), 208–221. zbl MR doi
[28] *M. Feistauer, V. Kučera, K. Najzar, J. Prokopová*: Analysis of space-time discontinuous Galerkin method for nonlinear convection-diffusion problems. Numer. Math. *117* (2011), 251–288. zbl MR doi
[29] *M. Feistauer, V. Kučera, J. Prokopová*: Discontinuous Galerkin solution of compressible flow in time-dependent domains. Math. Comput. Simul. *80* (2010), 1612–1623. zbl MR doi

[30] *M. Á. Fernández, M. Moubachir*: A Newton method using exact jacobians for solving fluid-structure coupling. Comput. Struct. *83* (2005), 127–142. doi
[31] *L. Formaggia, F. Nobile*: A stability analysis for the arbitrary Lagrangian Eulerian formulation with finite elements. East-West J. Numer. Math. *7* (1999), 105–131. zbl MR
[32] *L. Gastaldi*: A priori error estimates for the arbitrary Lagrangian Eulerian formulation with finite elements. East-West J. Numer. Math. *9* (2001), 123–156. zbl MR doi
[33] *J. Hasnedlová, M. Feistauer, J. Horáček, A. Kosík, V. Kučera*: Numerical simulation of fluid-structure interaction of compressible flow and elastic structure. Computing *95* (2013), S343–S361. MR doi
[34] *K. Khadra, P. Angot, S. Parneix, J.-P. Caltagirone*: Fictiuous domain approach for numerical modelling of Navier-Stokes equations. Int. J. Numer. Methods Fluids *34* (2000), 651–684. zbl doi
[35] *T. M. Richter*: Goal-oriented error estimation for fluid-structure interaction problems. Comput. Methods Appl. Mech. Eng. *223/224* (2012), 28–42. zbl MR doi
[36] *D. M. Schötzau*: hp-DGFEM for parabolic evolution problems: Applications to diffusion and viscous incompressible fluid flow. Thesis (Dr.Sc.Math)–Eidgenoessische Technische Hochschule Zürich, ProQuest Dissertations Publishing, 1999. MR
[37] *D. Schötzau, C. Schwab*: An *hp* a priori error analysis of the DG time-stepping method for initial value problems. Calcolo *37* (2000), 207–232. zbl MR doi
[38] *V. Thomée*: Galerkin Finite Element Methods for Parabolic Problems. Springer Series in Computational Mathematics 25, Springer, Berlin, 2006. zbl MR doi
[39] *M. Vlasák, V. Dolejší, J. Hájek*: A priori error estimates of an extrapolated space-time discontinuous Galerkin method for nonlinear convection-diffusion problems. Numer. Methods Partial Differ. Equations *27* (2011), 1456–1482. zbl MR doi
[40] *Z. Yang, D. J. Mavriplis*: Unstructured dynamic meshes with higher-order time integration schemes for the unsteady Navier-Stokes equations. 43rd AIAA Aerospace Sciences Meeting and Exhibit. Reno, 2005, AIAA Paper, 1222. doi

Authors' addresses: *Monika Balázsová*, *Miloslav Feistauer*, *Martin Hadrava*, *Adam Kosík*: Charles University, Faculty of Mathematics and Physics, Sokolovská 83, 186 75 Praha 8, Czech Republic, e-mail: balazsova@karlin.mff.cuni.cz, feist@karlin.mff.cuni.cz, martin@hadrava.eu, adam.kosik.cz@gmail.com; *Jaromír Horáček*: Institute of Thermomechanics, Academy of Sciences of the Czech Republic, Dolejškova 5, 182 00 Praha 8, Czech Republic, e-mail: jaromirh@it.cas.cz.